Thermal State of Permafrost in Central and Western Spitsbergen 2008-2009

Master's Thesis

Faculty of Science

University of Bern

Presented by

Zoé Lucia Lüthi

2010

Supervisor:

Prof. Christian Schlüchter
Institute of Geology, University of Bern
and Oeschger Centre for Climate Change Research

Co-Supervisor:

Prof. Hanne Christiansen
Institute of Geology, University Centre of Svalbard (UNIS)

Advisor:

PD Dr. Frank Preusser
Institute of Geology, University of Bern
and Oeschger Centre for Climate Change Research

Abstract

This 30 ECTS master's thesis focuses on the different ground thermal regimes at two study sites on Spitsbergen, Svalbard. According to results of the Permafrost and Climate in Europe (PACE) project, permafrost terrains have been exposed to atmospheric warming since 1975 with greatest warmside deviations at the borehole located on Svalbard. As part of an effort to understand the regional and local response of frozen ground to climate change, the present study assessed the impact of meteorology and of site-specific factors, e.g. vegetation and snow cover, on ground temperatures. An understanding of permafrost conditions in Spitsbergen is important for the management of terrain stability in areas of increasing population, and for predictions of potential climate change effects on the environment. Thermal time series of four boreholes in central and in western Spitsbergen where chosen to represent lowland dry and wet soils at a continental and at a maritime location over an annual cycle. For the first time, a complete hydrological year of ground thermal data at all selected study sites could be analyzed in autumn 2009. The thermal regimes of the four boreholes were first analyzed vertically and then compared on a regional and on a local scale. Results showed that the snow cover and duration exert a considerable influence on ground thermal regimes. In contrast, the results did not show any significant impact on ground temperatures by vegetation cover. Low surface offsets and direct atmosphere-ground coupling characterize the barren surfaces at the analyzed localities. The maritime dry ground displays the highest temperatures at the top of the permafrost (TTOP) and the greatest active layer thickness (ALT) whereas the lowest permafrost temperatures and the shallowest ALT were detected at the dry continental site. The implications of these results for understanding the impact of climate change in the High Arctic region are discussed.

Contents

1 Introduction

In the context of global climate change, Arctic ecosystems are of special interest due to their sensitivity to altered meteorological parameters and their potential to affect the global climate system through positive feedback mechanisms (ACIA, 2005; IPCC, 2007). Observations of thermal profiles in permafrost indicate that a significant temperature increase has been occurring in ground and air temperatures throughout northern Alaska, western Canada, the Siberian Arctic, northern Scandinavia and Svalbard over the last few decades (Overpeck et al., 1997; Serreze et al., 2000; Isaksen et al., 2007). The evidence from Svalbard is, however, only based on temperature observation from one deep borehole established by the Permafrost and Climate in Europe (PACE) project in 1998. Increasing mean annual air temperatures (MAAT) may affect regional climate patterns, the surface energy balance, active layer thickness and the hydrology of northern ecosystems (Hinzman and Kane, 1993; Waelbroeck, 1993; Chapin et al., 2005). In fact, the active layer thickness plays a crucial role in regulating biological, hydrological, geophysical, and biogeochemical processes through its effects on energy and mass fluxes between the surface and the atmosphere (Anisimov et al., 2002).

Further, permafrost thawing may release large stores of trace greenhouse gases, such as CO_2 and CH_4, found in frozen land areas into the atmosphere, thus leading to a positive feedback mechanism to global warming (Oechel et al., 2000; Christensen et al., 2004). However, not much attention had been devoted to permafrost in the High Arctic until frozen ground had been identified by the Global Terrestrial Observing System (GTOS) as one of the cryospheric indicators of global climate change within the WMO Global Climate Observing System (GCOS). Consequently, the Global Terrestrial Network for Permafrost monitoring program (GTN-P) was initiated by the International Permafrost Association (IPA) founded in 1983. GTN-P aims at collecting global long-term field observations to quantify current permafrost conditions and detect future changes. The network monitors active layer thickness and ground temperatures of permafrost areas at study sites throughout the Arctic (see Figure 1).

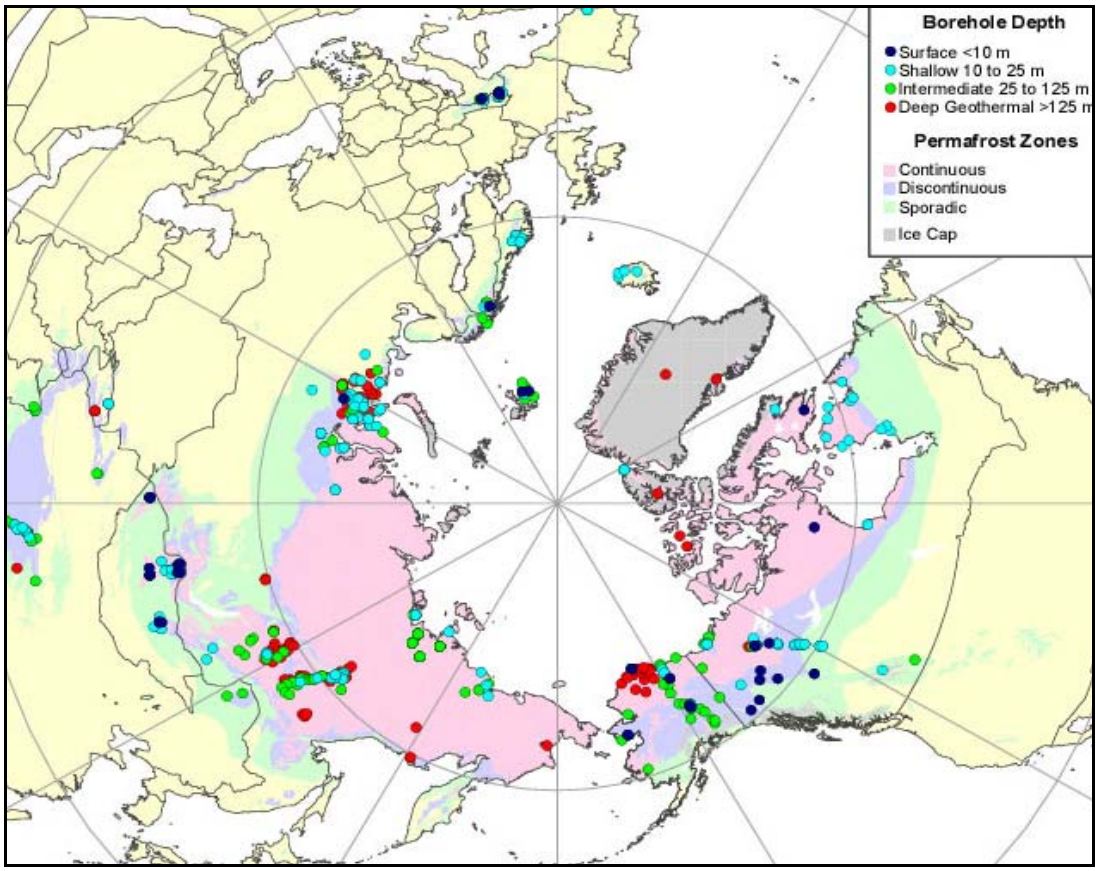

Figure 1 GTN-P borehole temperature monitoring sites in the Arctic. The permafrost distribution is represented by the different colors (source: www.farnorthscience.com).

Permafrost temperatures in Norway are monitored through the TSP NORWAY - Permafrost Observatory Project, a contribution to the Thermal State of Permafrost in Norway and Svalbard. The latter is an IPY research project that was established for the time period between 2007 and 2010. The project data is available online on the Norwegian Permafrost (NORPERM) database[1].

In addition, the responses of the active layer and of the near-surface permafrost to climate change are observed on a long time scale by the Circumpolar Active Layer Monitoring (CALM) network. Ground thaw progression measurements are performed in the Norwegian High Arctic at the UNISCALM site in Adventdalen by the University Center of Svalbard (UNIS).

[1] http://www.ngu.no/kart/permafrost/?lang=English

Svalbard, in particular has an interesting setting. This High Arctic region differs from sites at the same latitude elsewhere because of its influence by the Norwegian Current, a branch of the North Atlantic Current that is known to be highly sensitive to climate change (Førland et al., 2009a).

Increasing mean annual air temperature projections for Svalbard are of the range of 3 and 8 °C for the Southwest and the Northeast respectively for the period of 2071-2090 relative to 1981-2000. Mean annual precipitations are forecasted to increase in average by 12 % on Svalbard (Førland et al., 2009b). Environmental implications of ongoing climate change may therefore be significant. To monitor these changes, eleven new boreholes were drilled and instrumented in spring and in autumn 2008 for continuous thermal monitoring, mainly in the region of Nordenskiöld Land, in central Spitsbergen. The depths of the holes range from 4 m to almost 40 m. Boreholes were made in both unconsolidated sediments and bedrock. The holes are located in different landforms with different meteorological conditions in order to detect regional and local differences in ground thermal regimes. In fact, significant variations in ground thermal conditions are known to occur even within small areas of uniform climate due to local factors (Brown et al., 1973; Smith, 1975).

In this thesis changes in the subsurface thermal gradient at different locations on Spitsbergen are analyzed over an annual cycle. The study is based on thermal time series from four TSP-Norway boreholes and on meteorological data series from weather stations situated closed to the boreholes. The study areas have been chosen in order to represent High Arctic environments with different meteorological influences and with similar topographic characteristics. Thus, boreholes on the lowland were chosen in order to avoid the thermal influence of 3-dimensionality effects typical for mountain areas. Consequently, the investigated study sites of Adventdalen and Endalen correspond to a “continental” cold and dry climate, especially in winter due to its location at an inner fjord district, which normally gets covered by sea-ice for several months a year (Major et al., 2001). Kapp Linnè, on the other hand is characterized by a more “maritime” climate that is relatively mild and humid, partly because the sea around this area is normally ice-free.

The aim of the borehole selection from each study area was to characterize a location with “wet” ground and one with “dry” ground. This will illustrate the different response of close-by permafrost sites to the meteorological influence due to the influence of site-specific factors, such as vegetation growth and conductivity due to soil moisture. Landforms, such as solifluction sheets, raised beach ridge or loess terrace with its distinctive lithology will be taken into account, when comparing the thermal state of permafrost of the different study sites.

The thermal regime of the four boreholes are analyzed first on a vertical scale and then on a horizontal scale for local and regional comparisons. The aim is to parameterize the air-ground temperature relationship and to understand the influence of meteorology and local conditions on ground temperatures at the given study sites of the High Arctic region of Spitsbergen.

2 Scientific Background

In this section a short introduction to the expression of permafrost is given. The description of several terms used in the permafrost research leads the reader to a better understanding of the analyzed parameters presented later in the text.

2.1 Permafrost definition and distribution

Permafrost is defined on the basis of temperature. It is the ground (soil or rock) that remains at or below 0 °C for at least two years. Permafrost is not necessarily frozen, because the freezing point of the included water may be depressed several degrees below 0° C; moisture in the form of water or ice may or may not be present. Permafrost includes perennial ground ice, but not glaciers or bodies of surface water with temperature perennially below 0 °C. The thickness of permafrost may range from less than 1 m to more than 1000 m (Muller, 1943, van Everdingen, 1976, Kurdryavtsev, 1978. In: (Subcommittee, 1988)).

According to French (2007), more than 20% of the world's land area is underlain by permafrost. Perennially frozen ground occurs in high latitudes and high altitudes. Accordingly, French (2007) classifies permafrost into 1) latitudinal or polar permafrost, 2) alpine permafrost and 3) plateau or montane permafrost. Permafrost is typically classified in its extent as being continuous (90-100%), discontinuous (50-90%), sporadic (10-50%), or isolated (0-10%) (French, 2007); cf. Figure 1.

Permafrost in mid- and low- latitude mountains is to a large extent of the warm-type and its distribution is closely related to characteristics of the land surface, such as slope gradient and orientation, vegetation patterns, and snow cover (Noetzli et al.; Lunardini, 1996; Isaksen et al., 2007).

Sub-sea permafrost occurs close to 0°C over large areas of the Arctic Continental Shelf, where it may have formed during the last glacial period on the exposed shelf landscapes (Hubberten et al., 2004; Rachold et al., 2007). In fact, submarine permafrost studies at the East Siberian Seas (Romanovskii et al., 2005) identified continuous permafrost in the more shallow waters, and discontinuous permafrost at the greater depth of the outer part of the shelf.

2.2 Seasonal frost and permafrost

The layer of ground between the surface and the permafrost that undergoes seasonal freezing and thawing is called the **active layer** (Subcommittee, 1988; French, 2007), (see Figure 2). The response of the active layer and near-surface permafrost to climate change over long (multi-decadal) time scales is observed by the Circumpolar Active Layer Monitoring program (CALM), established at over 125 sites in both hemispheres in the 1990s. The active layer thickness is measured in grids ranging from 1 ha to 1 km², at the end of the thawing season.

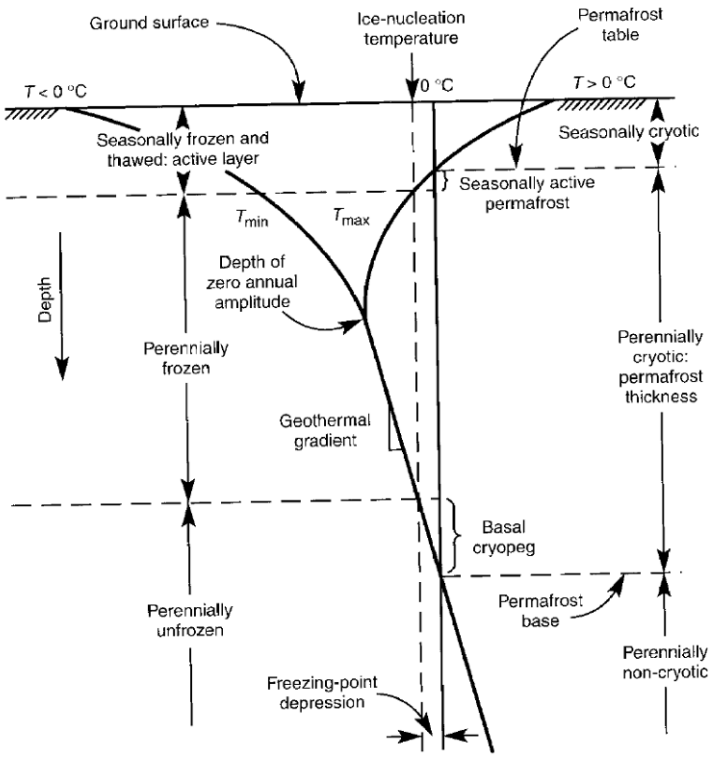

Figure 2 Definition of permafrost and active layer based on phase and temperature (after French 1996)

Typically pronounced in soils with high moisture content, the **zero curtain** represents a time period when the active layer shows a homogeneous temperature distribution close to 0 °C. In the autumn, for instance, the surface temperature drops sharply below 0 °C, and temperatures throughout the active layer fall to near 0 °C shortly after this. Subsequently, however, ground temperatures may fall slowly for a prolonged period, because large amounts of latent heat originating from the freezing of water within the active layer must be removed from the ground. The result is that the ground temperature remains near 0 °C for some period. This is terminated when most of the water is frozen, and rapid cooling then sets in (Smith and Riseborough, 2002).

The **Zero-Annual Amplitude** (**ZAA**) is represented by the depth at which the seasonal ground temperature fluctuations are less than 0.1 °C (Williams and Smith, 1989). The depth of ZAA may be 10-15 meters in soils, but can be much deeper in rocks (Williams and Smith, 1989). Permafrost temperature can vary considerably above the level of ZAA depending on air temperature and other factors such as drainage conditions and soil

properties (Hammer et al., 1985) but also further meteorological parameters, such as precipitation or wind.

The mean annual ground temperature at the depth where the maximum annual temperature is 0 °C is called **temperature at the top of permafrost** (**TTOP**). This temperature is used to calculate parameters such as the thermal offset, which is described below.

2.3 Site-specific parameters

If we imagine the ground surface as a thermal rather than a physical boundary, the mean annual temperature immediately above, at, and below the ground surface can be represented schematically (Williams and Smith, 1989), as illustrated in Figure 3. Three levels can be recognized (Smith and Riseborough, 2002): 1) air temperature, 2) ground surface temperature (MAGST) and 3) temperature at the top of permafrost (TTOP), also called the permafrost table. Thus, the **thermal offset** represents the difference between TTOP and MAGST. This parameter may not only vary temporally but also spatially. In fact, the change in soil thermal properties, e.g. porosity and moisture content, and the presence or absence of snow and vegetation cover lead to altering heat conductions (Hammer et al., 1985; Williams and Smith, 1989).

Moreover, between the ground surface and the top of permafrost, heat transfer by conduction varies seasonally between frozen and thawed states, since the thermal conductivity of ice is four times that of water (Smith and Riseborough, 2002). Thus, the higher thermal conductivity of the frozen active layer in winter that the thawed active layer in summer results in mean annual temperature at the permafrost table somewhat lower than the mean annual ground surface temperatures (Harris et al., 2009).

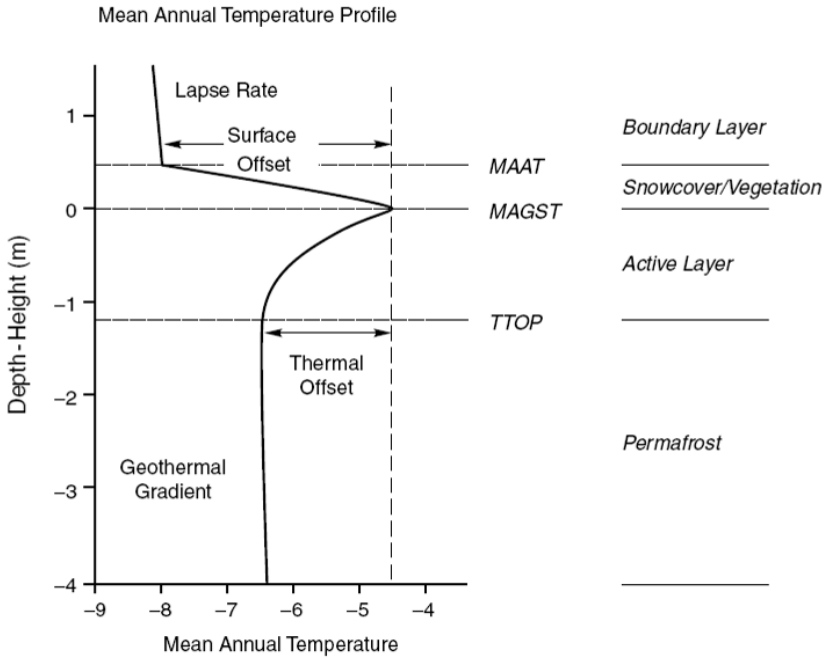

Figure 3 Schematic mean annual temperature profile through the surface boundary layer, showing the relation between air temperature and permafrost temperature (Smith and Riseborough, 2002).

The **surface offset**, also represented schematically in Figure 3, characterizes the difference between MAGST and MAAT. The insulation of winter snow cover, as described below for the nival offset, leads to higher MAGST compared to MAAT, whereas the effect of the vegetation offset leads to depletion in MAGST. However, generally the effects of snow cover in winter are greater than those of vegetation cover in summer leading higher values of MAGST than MAAT (Williams and Smith, 1989).

The **nival offset** is an expression for the combined effect of air temperature and snow depth. Thus, the temperature difference between the air and the ground surface is influenced largely by the presence of snow cover, which provides insulation. Snow accumulating in the fall can reduce the freezing in the winter, whereas snow falling in the late winter and spring can provide insulation against thawing in the spring (Hammer et al, 2004). Further, the low thermal conductivity of snow restricts the loss of heat from the ground during the coldest part of the year (Smith and Riseborough, 2002).

Vegetation can have an influence on the depth of the active layer and thus the upper level of the permafrost. The primary effect of vegetation is a reduction of solar radiation reaching the ground surface in summer, and thus depleting the energy source that can penetrate into the soil and thaw the frozen ground. In addition, interception and transpiration influence the ground thermal regime through the water balance (Smith and Riseborough, 2002). These effects are defined as **vegetation offset**.

The **N-factor** was first described by Lunardini (1978) as a transfer factor between air and ground surface temperature. Thus, seasonal thawing is parameterized by the scaling factor (n_t) between summer air and ground surface temperature that represents the vegetation effect. Whereas the scaling factor between winter air and ground surface temperature (n_f) represents the snow cover effect, thus, the value of n_f varies systematically with the mean winter snow depth and also with the mean annual air temperature (Smith and Riseborough, 2002). It is important to bear in mind that the value of the n-factor gets numerically smaller with increasing vegetation or snow influence on the ground surface temperatures.

Thawing or positive degree days (**DDT**) are calculated by summing up the average daily temperatures that are above zero centigrade, whereas the **freezing or negative degree days** (**DDF**) are the sum of the average daily temperatures below zero centigrade (Walker et al., 2008) during a hydrologic measurement year, i.e. 1st of September until 31st of August of the following year (Bruland et al., 2001). Degree days are calculated for the air temperature (AT) and accordingly DDTa, DDFa and for the ground surface temperature (GST) with the according symbols of DDTs, DDFs. These parameters give, according to the above cited author, a sense of the 'cold content' of winter and warmth of summer, and the calculations are not constrained by arbitrary dates that define the seasons, for example, calling June-July-August 'summer' This is particularly important since the timing of the beginning and the end of a season can vary from year to year.

3 Study area

3.1 The Svalbard archipelago

3.1.1 Geographical and geological setting

Figure 4 Map of the Svalbard archipelago (source: www.russia.no/regional/Svalbard/Svalbard-map-4.jpg).

Svalbard is an archipelago that stretches between 74°-81° N and 10°-35° E. It covers about 63.000 sq. km. The main area consists of the Spitsbergen group, where Spitsbergen is the largest island (39.000 sq. km), followed by Nordaustlandet (15.000 sq. km), Edgeøya (5.000 sq. km), Barentsøya (1.300 sq. km) and many smaller islands.

Nordendskiöld Land is the region that hosts the main settlement called Longyearbyen; the area is located in central Spitsbergen. The highest peaks in Svalbard, Newtontoppen (1713 m) and Perriertoppen (1712 m), are situated in northeast Spitsbergen.

About 60% of the archipelago is covered by polythermal glaciers, with a significant increase in glacier cover from West to East. In Svalbard permafrost is continuous outside the areas covered by glaciers, however frozen ground extends beneath cold-based glaciers and the margins of polythermal glaciers. Permafrost thickness ranges from about 70 m near the coast to over 500 m in the highlands (Liestøl, 1976). Permafrost development on Svalbard was apparently controlled by Holocene cooling after around 3 ka BP (Svensson, 1969; Jeppesen, 2001).

Svalbard has an extremely varied geology, representing all main periods from Precambrian to Quaternary. The sparse plant cover, moreover, facilitates geological investigations. The oldest formations are found as a belt along the west coast of Spitsbergen as well as in the northern part of Nordaustlandet, whereas the youngest rocks, of Tertiary age, are found in the central and southern parts of Spitsbergen (Hirsdal, 1985). Several areas of Svalbard are covered by sedimentary rocks, which often are rich in fossils. Volcanic activity is known to have occurred during the Quaternary period and it is presumed that Svalbard was buried and depressed by a large ice sheet during the course of the last ice age,. Isostatic uplift following deglaciation created marine terraces to be found up to 130 m above the present sea level. It is further maintained that the sea bed of the Barents Sea also was covered and depressed by ice.

3.1.2 Ocean currents and sea ice

The Norwegian Current, a branch of the North Atlantic Current, transports warm water masses (i.e. Atlantic water) into the Barents Sea and along the western coast of Spitsbergen, as represented in Figure 5.

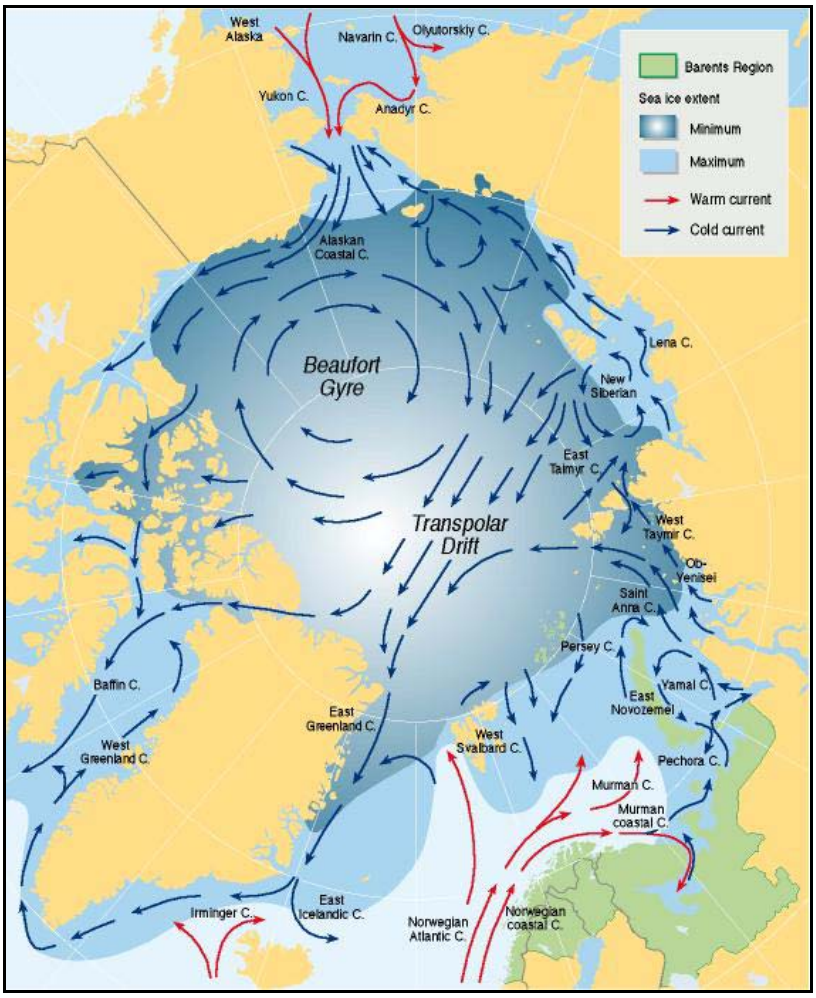

Figure 5 Ocean currents and sea ice extent (from AMAP).

According to Dickson et al. (2000), a close correlation exists between the North Atlantic Oscillation (NAO), the Arctic Oscillation (AO) and long-term changes in the strength and water temperature of the Fram Strait and the Barents Sea inflow branches. Whether or not these processes impact sea-ice conditions or extent remains controversial.

Understanding these links is important because changing sea-ice conditions contribute to the large climate variability at the Norwegian high-Arctic weather stations described below, especially during winter (Førland et al., 2009b).

3.1.3 Climate and meteorology on Svalbard

The Svalbard archipelago shows similar Holocene climate fluctuations as the rest of Arctic Scandinavia (André, 1997). Paleoclimatic conditions have been reconstructed

using several methods. For example, radiocarbon dating of whale bones and driftwood indicate that deglaciation of the investigated fjords in central Spitsbergen occurred between 13 and 10 ka BP (Corbel, 1966; Forman and Miller, 1984). Sediment cores from the Nordic Seas near Svalbard indicate that the first half of the Holocene may have been the warmest period since the last 13.4 ka (Koç, 1993). The early Holocene warming appears to have culminated between 9 and 6.5 ka BP according to δ18O data from the Barents Sea (Hjort, 1997; Ivanova et al., 2002). According to (Salvigsen, 2002), MAAT values 3-5 °C higher than today influenced the paleoenvironment until ca. 5 ka BP. The warm period was then followed by a colder period with rock glacier formations (André, 1994) and glacier expansions. The latter reached a maximum in western Svalbard around 2.3 ka BP, whereas maximum Holocene cooling occurred during the Little Ice Age (Furrer, 1994; Humlum et al., 2005). MAAT was calculated for the LIA period to be 4-6 °C below late 20th century values; this is evidenced by the long composite meteorological record from Svalbard (Harris et al., 2009). The contemporary climate amelioration began at the end of the last century and culminated in the late 1930s (André, 1997). Nordli and Kohler (2004) claim that as much as 2/3 of the winter warming from the 1910s to the 1920s can be explained by an increase of cloud cover recorded at the Green Harbour and at the Longyerabyen meteorological station.

The Norwegian high-Arctic weather stations are all coastal stations located on Spitsbergen, Hopen, Bjørnøya and Jan Mayen. Spitsbergen includes the station of Longyearbyen/ Svalbard Airport, Isfjord Radio at Kapp Linnè, Ny-Ålesund, Green Harbour/ Barentsburg, Svea and Hornsund.
The meteorology has been particularly well-documented in Longyearbyen since 1912 (Førland et al., 1997) and it is the longest meteorological series from the High Arctic.

Svalbard lies in the border zone between cold Arctic air from the North and mild maritime air form the South at a great pressure gradient zone of the polar front. This setting is particularly prone to cyclonic activity, especially in winter, when the weather often is unstable and stormy. The prevailing winds on Spitsbergen are from the northeast-southeast sector (Hanssen-Bauer et al., 1990 ; Førland et al., 1997). Yet, the shifting polar

front makes the Norwegian arctic stations exposed to air masses of very different origin. This is also a reason why these stations show rather large climate variability in spite of their coastal environments.

There is a strong temperature gradient over Spitsbergen extending from southwest to northeast. The average temperatures vary from -10 °C along the west coast to below -20 °C in the north-east during the winter months. January-March is normally the coldest period of the year. However, even during these months, above-zero temperatures have been recorded at all stations. Considerably smaller contrasts are recorded in summer, when the temperatures during the warmest months are around 4-6 °C. Maximum temperatures rarely exceed +15 °C, yet temperatures above 20 °C have occasionally been recorded at Svalbard Airport (Førland et al., 2009b). Strong temperature fluctuations are indices for the high climatic sensitivity of Svalbard (Houghton et al., 2001). This sensitivity is evidenced by the marked warming in surface air temperature around 1920, which has been mentioned earlier; this temperature increase was then followed by a sharp drop in air temperatures by about 5 °C from 1957 to 1968, with a subsequently more gradual increase towards the end of the 20th century (Humlum et al., 2003).

Førland et al., (2009b) state that precipitation is usually low in the High Arctic because air masses often are stable stratified and contain only small amounts of water vapor. The normal (1961-1990) annual measured precipitation in the Svalbard region is 190-440 mm. Precipitation is at maximum during autumn and winter. Similar to the above mentioned temperature values; there is a gradient over Spitsbergen from high values in the southwest to lower values in the northeast in all seasons except during summer. The mountain region on Spitsbergen gets the greatest amount of precipitation, whereas the least is recorded at the inner fjord district; however considerable local differences are caused by topography. It should be stressed that reliable measurements of precipitation are difficult to obtain under certain harsh weather conditions (Førland et al., 2009b).

3.2 Field sites in central and western Spitsbergen

There are considerable climatic differences between the Longyearbyen area and Kapp Linnè (Ohta et al., 1992). Longyearbyen / Svalbard Airport is the closest Norwegian high-arctic weather station to Adventdalen and it shows one of the most continental climates among the stations on Spitsbergen. The winter temperatures are 2-5° C lower, and the summer temperatures 1-2° C higher than at the coastal station at Isfjord Radio, Kapp Linnè (Førland et al., 2009b).

The frequent presence of open water creates a climate at Isfjord Radio that is more coastal or maritime than any other Spitsbergen station (Hanssen-Bauer et al., 1990).

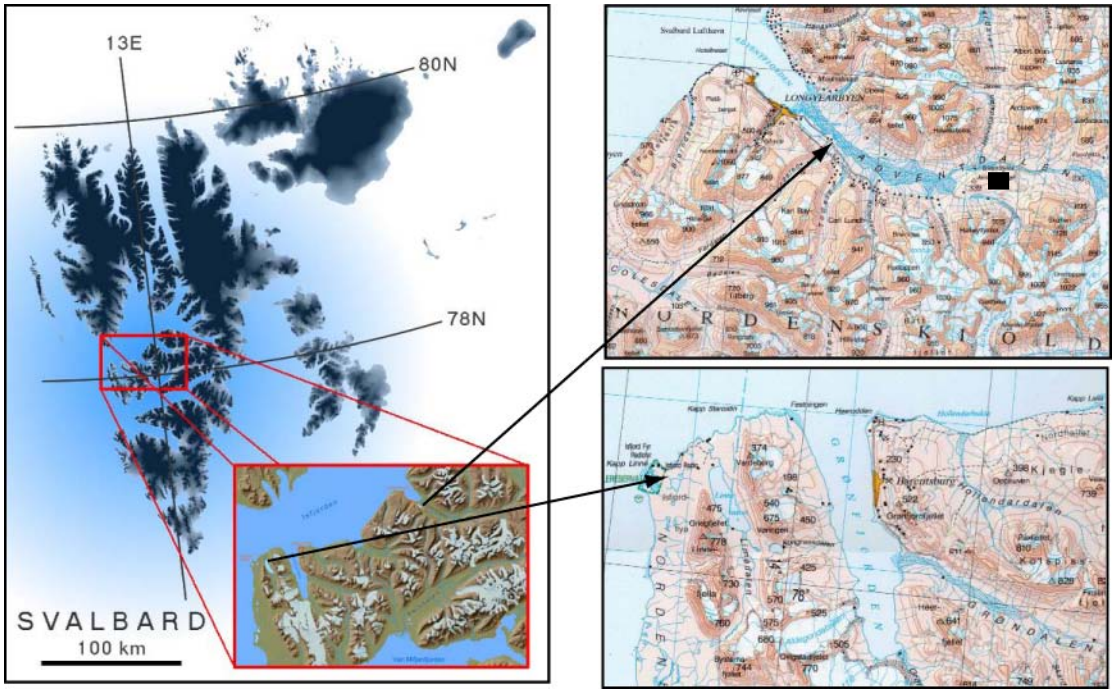

Figure 6 Study sites. The figure on the left represents the enlarged region of Nordenskjöld Land. The maps on the left hand site illustrate the continental location of Adventdalen and Endalen at the top and the maritime influenced site of Kapp Linnè at the bottom. The black rectangle at the top-right marks the location of the PACE borehole on Janssonhaugen, Svalbard (from OziMap).

3.2.1 Adventdalen and Endalen

Adventdalen is one of the major glacial valleys in the northeastern part of Nordenskiöld Land. It has a wide and flat floor with a network of braided river channels and alluvial

plains. The river of Adventelva drains into Adventfjorden, a small fjord that extends south of Isfjorden.

The valley is surrounded by large mountain plateaus, which are formed in horizontal-lying sedimentary rock. The oldest rocks are of Permian, the youngest are of Tertiary age (1972). The unconsolidated deposits at the floor of the valley consist of marine shore deposits and fluvial and glaciofluvial deposits (Major et al., 2001). Marine sediments and relict beach ridges are found up to 5 km from the coast of Adventfjorden at about 25 m a.s.l. (Tolgensbakk et al., 2000).

Endalen is a v-shaped tributary valley of Adventdalen. It shares the same hard-rock geology and similar meteorology like Adventdalen.

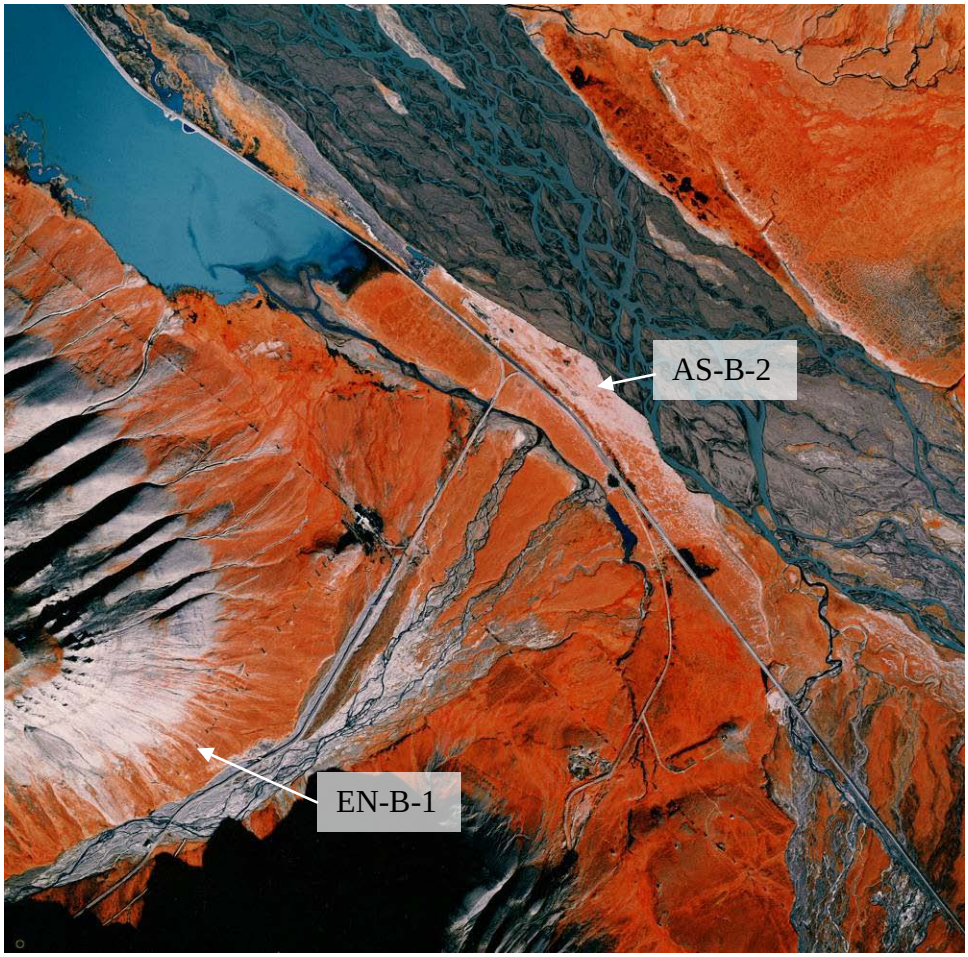

Figure 7 Aerial photography (1: 15000) of the study sites in Adventdalen and in Endalen. AS-B-2 and EN-B-1 represent the boreholes at the dry and at the wet location respectively (from: Norwegian Polar Institute, 1990).

The analyzed borehole in Adventdalen is located on a loess terrace, between the circumpolar active layer monitoring site and an international monitoring site called Old Auroral Station. We therefore named the borehole Old Auroral Station 2 (AS-B-2), since it is the second of the boreholes that were drilled at this site. The fact sheet for the borehole is represented in the table below.

Table 1 Fact sheet of the AS-B-2 borehole.

Acronym	AS-B-2
Location	Latitude: 78° 12' 05"; Longitude: 15° 50' 04"; Altitude: 9 m a.s.l.
Topography	Plain
Surface material	Aeolian material
Vegetation	Tundra, mainly Salix and grasses but very sparse
Snow condition	Thin snow thickness (less than 30 cm)
Lithology	0-1.2m: sand with some gravel, 1.2-3m: sand/silt/clay, 3-4m: ice, 4-6m: mainly clay/silt, 6-10m: clay/silt, possibly some sand
Sensor depths	0.00; -0.25; -0.50; -0.75; -1.00; -2.00; -3.00; -5.00; -7.00; -9.85 m

As discussed later on, the stratigraphy of the ground is not well recorded due to the applied method of drilling, which was carried out with the hammer drilling method. This is the case for all four analyzed boreholes.

AS-B-2 is the “dry” site of permafrost monitoring in Adventdalen, with little snow and vegetation cover. Endalen, on the other hand, was chosen to depict a more “wet” site of permafrost monitoring. The borehole EN-B-1 is situated next to a solifluction measurement station, since this site is subject to slope movement. Its site-specific factors are listed below.

Table 2 Fact sheet of the EN-B-1 borehole

Acronym	EN-B-1
Location	Latitude: 78° 11' 25"; Longitude: 15° 46' 53"; Altitude: 53 m
Topography	Slope
Surface material	Solifluction material
Vegetation	Lichen, mainly mosses but also Cassiope, Salix, Dryas and grasses
Snow condition	Moderate snow thickness (between 30 and 80 cm)
Lithology	0-1.5m: diamictite: high fraction of fine material and scattered blocks; 1.5-2m: coarser material with ice lenses (10-20cm); 2-4m: diamicton with blocks and finer material (silt/clay), some ice lenses (3-4cm thick); 4-5m: diamicton, drier than above from 4.5m; 5-6m: transition to bedrock; 6-20m: bedrock, solid from 7.7m.
Sensor depths	0.00; -0.25; -0.50; -0.75; -1.00; -1.50; -2.00; -2.50; -3.00; -4.00; -5.00; -6.00; -7.00; -8.00; -9.00; -10.00; -12.00; -15.00; -19.00 m

EN-B-1 has online data transfer via GSM. Thus, data series can be viewed and downloaded, just like the meteorological data from different monitoring sites, such as the Old Auroral Station.

The mean annual air temperature in the Longyearbyen area was -6 °C for the period 1961-1977, and -6.7 °C between 1975 and 1990. Whereas the annually measured precipitation value (MAP) was 210 mm and 190 mm for the two periods respectively (eklima.no 2009). There are two periods for the normal (mean temperature value) in the Longyearbyen area, due to a shift in the operating weather station, from the old Longyearbyen station that closed down in 1977, to the now operating Svalbard airport weather station.

The low precipitation of this area leads to relatively moderate snow accumulation during the winter. Its distribution, however, varies depending on local conditions such as topography and exposition related to wind direction. While some areas are blown completely free of snow, other areas can accumulate up to several meters of snow.

The prevailing wind direction in this area is southeast.

3.2.2 Kapp Linnè

Kapp Linnè is situated at the northwestern tip of Nordenskiöld Land. To the north lies Isfjorden, to the west the open sea and to the east and southeast a mountain range with heights up to 600-800 m.

This area south of Isfjorden shows one of the best exposed, almost continuous coastal sections of Late Permian through the lowermost part of the Tertiary strata. The exposed bedrock around Kapp Linnè consists mainly of diamictite that is largely covered with marine shore deposits (Ohta et al., 1992). Ice- and soil-wedges create a system of sorted and unsorted polygons on the strandflats and raised beach ridges. These periglacial landforms are indices for permafrost occurrence throughout the area, including the coastline, where ice-wedge polygons were traced out (Åkerman, 1980). Moreover, block fields, sorted circles and sand dunes also contribute to this periglacial environment. The exact depth of the permafrost is not known because no deeper borings have been made in this area, however, it is clear that great variations in permafrost thickness are present at the Kapp Linnè location, ranging between 75 and 450 meters (Liestøl, 1976; Liestol, 1977). There are several lakes that are surrounded to a great extend by bog areas.

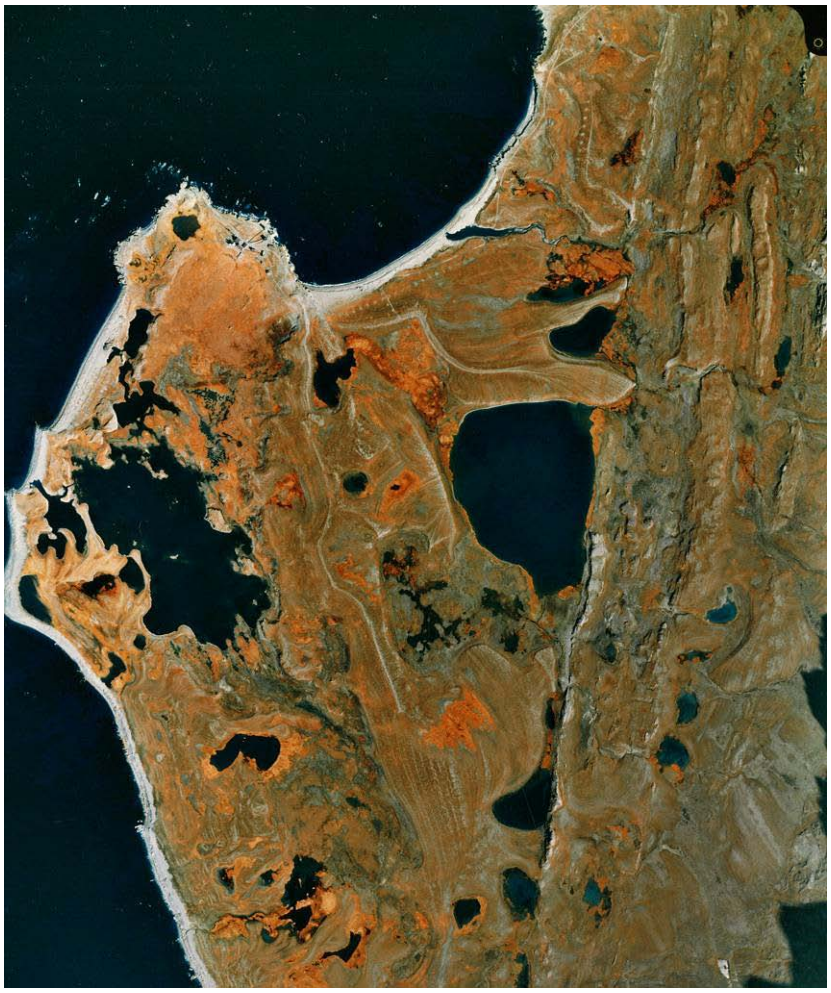

Figure 8 Aerial photography (1: 15000) of the study sites at Kapp Linnè. KL-B-2 and KL-B-3 indicates the boreholes at the dry and at the wet location respectively (from : Norwegian Polar Institute, 1990).

Even though the mean annual precipitation at Kapp Linnè is higher than in Adventdalen, barren surface is very common in winter, since snow tends to accumulate only in a few spots due to the strong wind action in this area. The latter is strengthened locally by Isfjorden, which is narrower at the mouth than further in (Førland et al., 2009b). The prevailing wind direction is east, northeast (Hanssen-Bauer et al., 1990). MAAT at the Isfjord weather station was -5.1 °C during the period of 1961-1990, and MAP for the same time interval was 480 mm[2]. Kapp Linnè is known to be an overcast area, especially in summer when low clouds are very common. Winters tend to be milder than in the Longyearbyen area due to the maritime influence of the open sea.

[2] www.eklima.no , accessed: September 2009

The chosen borehole for the dry permafrost environment in this area is located on a raised beach ridge; it is the deepest of our boreholes; c.f. Table 3.

Table 3 Fact sheet of the KL-B-2 borehole

Acronym	KL-B-2
Location	Latitude: 78° 3' 15.876"; Longitude: 13° 38' 13"
Topography	Plain
Surface material	Beach ridge sediments
Vegetation	No vegetation
Snow condition	Thin snow thickness (less than 30 cm)
Lithology	0-2m: coarse (gravel) beach deposit (dry beach ridge); 2-4.8m: sand and clay, some occurrences of silt, cohesive; 4,8-6,2m: fine gravel; 6,2-38m: bedrock
Sensor depths	0.00; -0.25; -0.50; -0.75; -1.00; -1.50; -2.00; -2.50; -3.00; -4.00; -5.00; -6.00; -7.00; -8.00; -9.00; -10.00; -12.00; -15.00; -20.00; -25.00; -30.00; -35.00; -38.00 m

The borehole that represents the wet permafrost area is situated some 50 m to the South of KL-B-2, in a bog area. Its characteristics are listed in Table 4 below.

Table 4 Fact sheet of the KL-B-3 borehole

Acronym	KL-B-3
Location	Latitude: 78° 3' 11" ; Longitude: 13° 38' 23
Topography	Plain
Surface material	Bog
Vegetation	Mosses and grasses
Snow depth	Moderate snow thickness (between 30 and 80 cm)
Lithology	0-1.2m: organic matter with sand and ice; 1.2-2m:sand and silt/clay, beach sediment partly unfrozen; 2-4m: layered sand with gravel and shells (20cm thick); 4-6m:fine sand with shells, drier; 6-8m: well graded sand; 8-10m: coarse gravel with sand
Sensor depths	0.00; -0.25; -0.50; -0.75; -1.00; -1.25; -1.50; -2.00; -3.00; -4.00 m

KL-B-3 was drilled down to 10 m but only the upper 4 m could be installed with a thermistor string because the lower part of the borehole had collapsed.

4 Instruments and methods

4.1 Meteorological data

The main station at Kapp Linnè is called Isfjord Radio, established some 50 m from the sea on a flat raised beach ridge, 7 m a.s.l. The weather station was established in 1934; it was then destroyed during World War II in 1941 and reestablished in 1946. Unfortunately no regular observations have been available for scientific purposes during the last years. To rectify this situation, a Mini Temperature Data logger (MTD) has been installed in a so-called English hut, a small elevated house, situated next to the main station. In this thesis the air temperature data from the above mentioned minilogger is analyzed for the time interval of interest, i.e. 27th of September 2008 until 26th of September 2009.

Normal MAAT and MAP values for the period 1961-1990 were calculated with data series from the official meteorological station of Isfjord Radio and from the airport at Longyearbyen for the Adventdalen study site. These data series were retracted from eKlima, a database that offers free access to weather- and climate data from the Norwegian Meteorological Institute.

Data series for the air temperature at the study site in Adventdalen and in Endalen were taken from the weather station in Adventdalen. The latter is situated on the loess terrace next to the CALM site, 19 m a.s.l.. This station has been operating since 1993, and was replaced by a taller mast in April 2009. We therefore talk about data from the old- and the new weather station of Adventdalen. These data series are available on the UNIS website.

4.2 Ground temperature data

The logging of ground temperatures over time is achieved with soil temperature sensors situated in borehole temperature measuring chains, also called thermistor strings.

The boreholes were drilled during the winter season with a hammer drillrigg that had to be transported to the field site as long as the surface was frozen, in order to minimize the

impact on the ground. The material that was brought up to the surface was analyzed and the different layers were determined as good as possible since the ground was crushed with the hammer drillrigg.

A protective plastic tube with 5 cm diameter was then lowered into the borehole. For environmental reasons the tube was not filled with any liquid like fuel, which would most likely give a better picture of the ground thermal conditions. The bottom of the tube is sealed, whereas the upper end is placed in a plastic casing that protects the data logger instrumentation. This casing is installed a few meters beside the borehole so as not to disturb the natural temperature progression.

The compact instrumentation that allows precision measurements in harsh environments were ordered from the Swiss company AlpuG (ALPine natUral danger)[3], a reseller of the Campbell Scientific UK Company. The purchased CR800 series data logger has a temperature-resistant battery that consumes minimal power and is therefore ideal for autonomous monitoring systems at field sites in harsh environments.

The more shallow boreholes AS-B-2 and KL-B-3 were instrumented with digital temperature strings from the Geoprecision Company[4] that are attached to a mini-data logger, installed directly at the upper end of the casing tube.

The temperature of these two boreholes is registered every hour with an accuracy of +/- 0.2 degrees, whereas EN-B-1 and KL-B-2 have a time interval of 6 and 2 hours respectively at an accuracy of +/- 0.02 degrees.

It is important to keep in mind that the sensors were placed at the required depths during the installation of the thermistor strings, for instance at 0 cm depth for the ground surface temperature, but we can not exclude slight errors in particular due to the uneven surfaces.

[3] http://www.alpug.ch/ , 2009

[4] http://www.geo-precision.com/ ,2009

4.3 Data collection

The permafrost borehole temperature measurements get collected at the monitoring sites several times a year. The connection between the CS I/O and RS-232 serial ports of the Campbell data loggers allows transferring the data to the notebook. Apposite software for the RS interface was previously installed on the computer, whereas the communication interface for the Geoprecision data loggers M-Log7 is an infrared interface through which the data gets downloaded on the notebook with the apposite software.

The temperature data of the boreholes (see Figure 9) is then uploaded on the NORPERM database[5] .

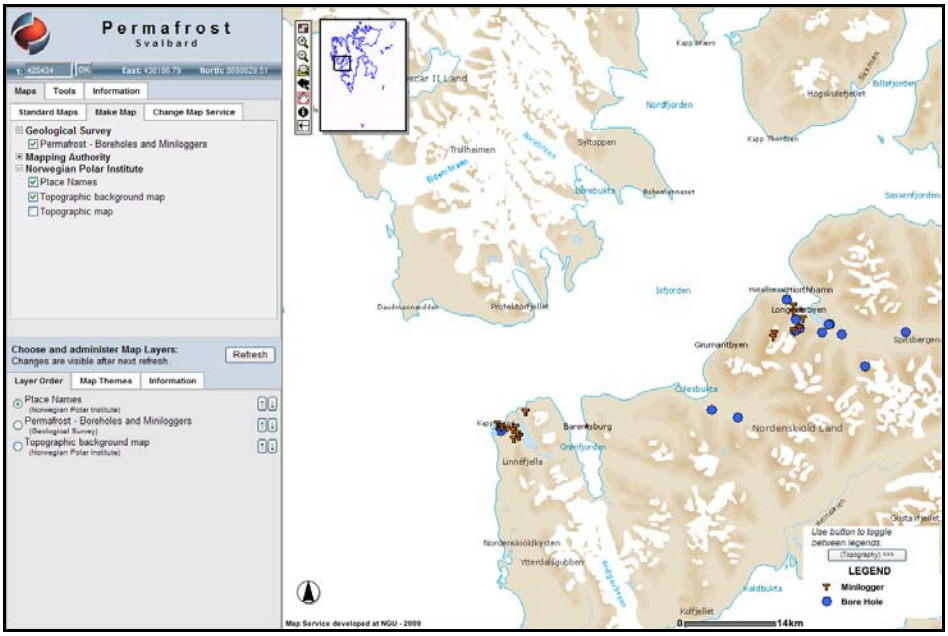

Figure 9 NORPERM Database interface showing the location of the boreholes and the mini loggers.

One full year of data for each of the four analyzed sites was completed on the 24th of September 2009. However, due to the thermometric lag, the required time for the sensors to come to equilibrium with the natural temperatures of the soil after their installation, the 28th of September 2008, has been chosen to represent the starting date and the 27th of September 2009 was chosen for the ending date for the analysis in this thesis. It has been taken into consideration that this period does not exactly correspond with a hydrologic

[5] www.ngu.no/kart/permafrost_svalbard/, 2009

measurement year, which, according to standard procedures, is the preferred observation period. Additionally, the ground temperature data from the borehole in Adventdalen had to be shifted six days ahead, thus the period is here 19.09.2008-18.09.2009.

Surface conditions, including winter snow depth, vegetative species composition and density, and organic layer depth around the boreholes were evaluated through field observations. These site-specific factors are important to establish physical differences between the study sites.

4.4 Data analysis

Standard parameters (MAAT, MAGST, ALT, TTOP, Degree Days, N-factors, thermal and surface offsets) were calculated in order to make a comparison between the different sites. Therefore, temperatures at different depths were averaged into daily values and plotted against time. As stated above, the period was chosen appositely to represent a full measurement year at all the study sites. There are a few data gaps due to measurement failures.

To have a first idea of the ALT and the changes in the subsurface thermal gradient over an annual cycle, the thermal regime for the study period was calculated, based on linearly interpolated temperatures between the different sensors. The plots were scaled to 4 m depth, which is the level to which the most shallow boreholes reaches. In this way a better comparison between the thermal regimes at the four study sites is possible.

Further, air temperatures recorded at Kapp Linnè and in Adventdalen were used to determine annual mean temperature and degree-day indices.

According to Smith and Reiseborough (2002), MAAT and MAGST can be expressed in terms of AT and GST degree-day sum, respectively:

(1) $$MAAT = \frac{DDTa - DDFa}{P}$$

(2) $$MAGST = \frac{DDTs - DDFs}{P}$$

Seasonal thawing (n_t) and freezing (n_f) n-factors have been calculated from GST and AT time series following Lunardini (1978):

$$n_f = \frac{DDFs}{DDFa} = \frac{\int_0^{\theta_{fs}} (|GST| - T_f)dt}{\int_0^{\theta_{fa}} (|AT| - T_f)dt} \quad (3)$$

$$n_t = \frac{DDTs}{DDTa} = \frac{\int_0^{\theta_{ts}} (GST - T_f)dt}{\int_0^{\theta_{ta}} (AT - T_f)dt} \quad (4)$$

Offsets and the temperatures at the permafrost table were calculated after Smith and Riseborough (2002):

$$NivalOffset = \frac{DDFa(1 - n_f)}{P} \quad (5)$$

$$VegetationOffset = \frac{DDTa(1 - n_t)}{P} \quad (6)$$

$$TTOP = MAAT + SurfaceOffset + ThermalOffset \quad (7)$$

$$SurfaceOffset = MAGST - MAAT \quad (8)$$

$$ThermalOffset = TTOP - MAGST \quad (9)$$

The descriptions of the parameters are given in the section *Scientific Background*. In addition, a complete list of symbols used in this thesis is to be found in Table 6 in the appendix section.

Further, a number of plots were made in order to represent the regional and local differences of the ground thermal regime. The annual thermal cycle was plotted for the four study sites on a so-called Trumpet Curve. Therefore, the annual mean, minimum and maximum temperature was calculated for the data series of each sensor and then plotted

against depth. The thermal regime for 0.5, 1 and 10 m depth of each borehole was plotted against time. In addition, subsurface temperatures of the 9th and of the 24th of September 2009 were illustrated with different combinations of boreholes in order to show spatial differences.
All calculations and plots were made with the matlab program.

5 Results

In this section some graphs are displayed. The analysis of the vertical profiles is presented first, followed by the spatial comparison of thermal regimes. Nevertheless, more plots are to be found in the Annex section.

5.1 Continental sites

MAAT during the analyzed hydrological year of 2008-2009 was calculated as -5.29 °C. This value differs slightly for the AS-B-2 site, since the analyzed period had to be shifted one week ahead for the data series of this study site. The annual cycle of air temperature indicates that the coldest period took place between January and April 2009. However, a few days with plus-degrees occurred even during months with negative temperatures. The minimum daily air temperatures recorded during the analyzed period was -31 °C, while the maximum was +12 °C.

5.1.1 AS-B-2, dry location

The thermal regime for the borehole in Adventdalen AS-B-2 was calculated for the period 19/09/2008-18/09/2009. As mentioned above, this does not coincide exactly with the period of other three boreholes. MAAT during this period was -5.24 °C, while MAGST was -4.46 °C. Based on linear interpolation ALT was estimated at 0.94 m depth, with corresponding TTOP of -4.75 °C.

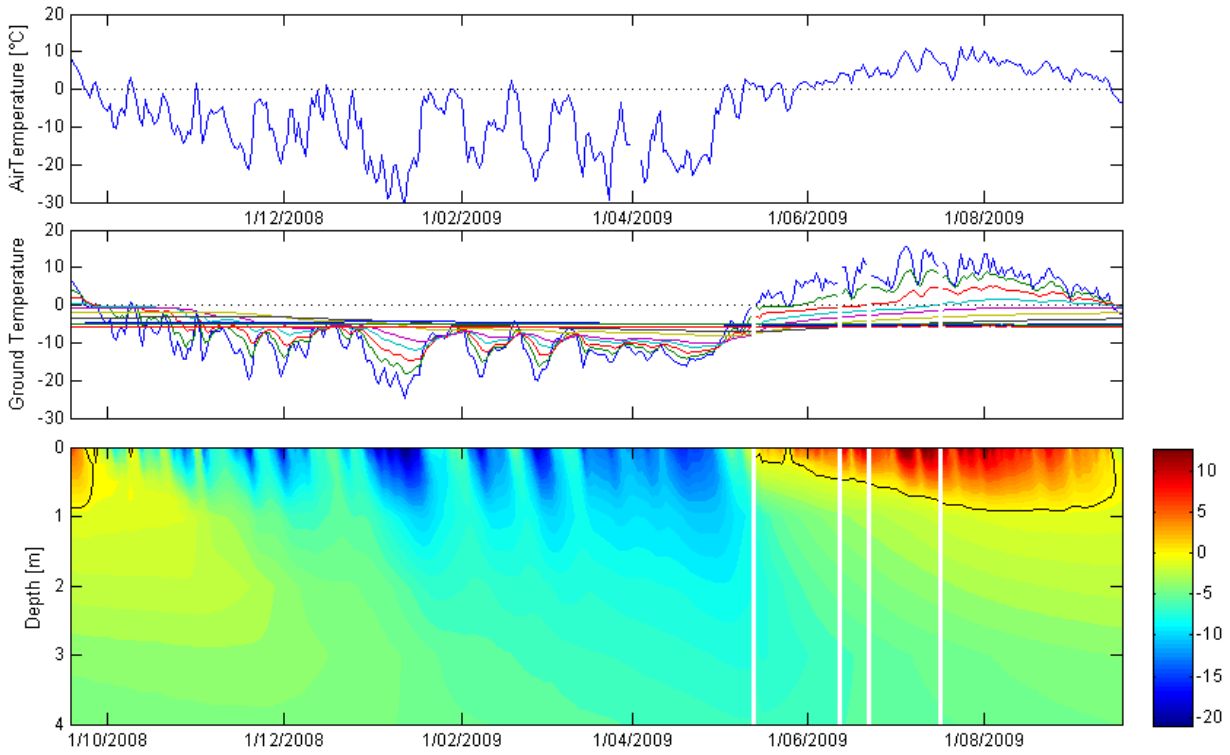

Figure 10 Thermal regime at the dry, continental site of AS-B-2. The uppermost plot represents the annual cycle of the air temperature, in the middle the ground thermal regime at the different sensors is represented with their linearly interpolated temperatures at the bottom. The black line indicates the 0-isotherme; the white stripes indicate data gaps due to instrumental failures.

AL thawing begins in the middle of May and ends at the end of September. It is interrupted by a short freeze-back of the sill shallow AL at the end of May, when air temperatures sharply dropped below 0 °C as seen in Figure 10.

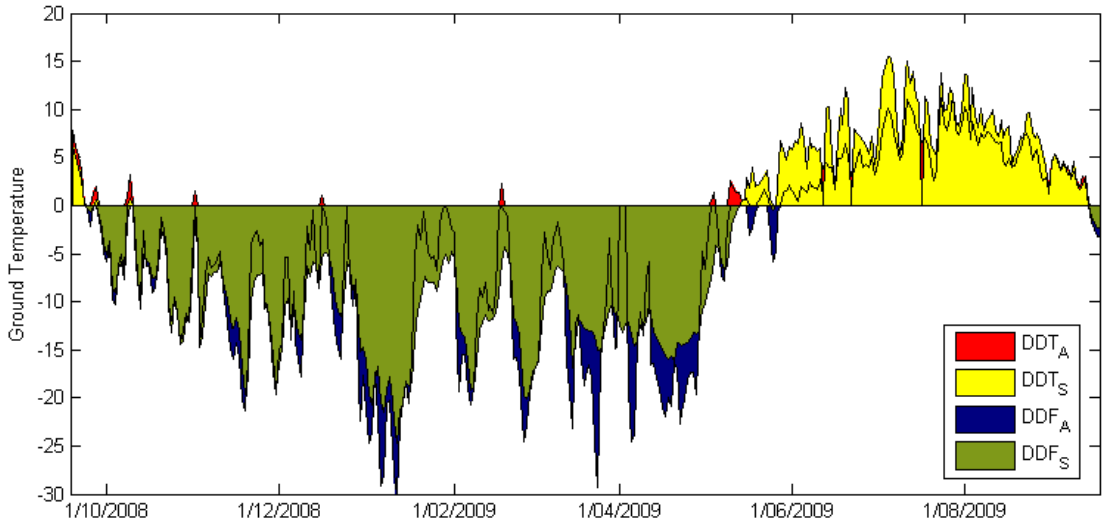

Figure 11 Degree-days of the air and of the ground surface at AS-B-2 illustrate the relation between AT and GST. DDTa and DDTs indicate the thawing degree-days of the air and of the soil respectively; DDFa and DDFs indicate the freezing degree-days of the air and of the soil respectively.

The thermal regime of the borehole clearly shows a close correlation between GST and AT, cf. Figure 11. The ground temperatures during the cold period, however, show a phase with somewhat less pronounced high-frequency temperature fluctuations than the air temperatures. This phase begins in March and lasts until the middle of May, when the upper part of the soil started to thaw. This phenomenon might be caused by the insulating effect of a snow pack that seems to have developed only late in the winter. On the other hand, GST of the warm period display more pronounced fluctuations than AT. This could be due to insolation directly hitting the casing tube with the sensors. A similar pattern is observed for KL-B-3 that has the same type of installation, as described later on.

Overall, the variation in near-surface temperatures diminished with depth. By contrast the phase-lag increases with depth, displaying thermal waves that are delayed by several days, which is also recognized at the other boreholes.

Conclusively, the high correlation between AT and GST at this site suggest low insulating effect of the snow in winter, and little or no buffering factor of the vegetation in summer. In addition, the fine-grained soil might enhance the energy conduction from the atmosphere into the soil.

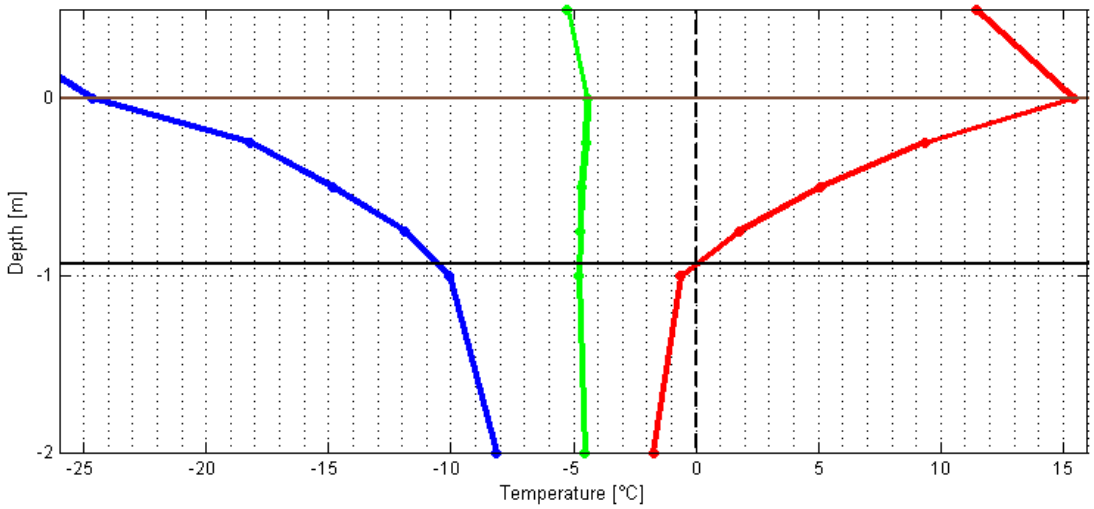

Figure 12 Minimum (blue), average (green) and maximum (red) thermal regime during the analyzed period of 2008-2009 at the AS-B-2 site. The black solid line indicates the ALT; the solid brown line indicates the ground surface; the solid dots indicate the depth at which the sensors are placed.

The mean surface offset at this site (e.g. Figure 12) was calculated as 0.78 °C. This parameter is probably influenced by the slight insulating effect of the shallow snow cover, which seems to be more important than the weak cooling effect of the vegetation. Thermal offset resulted in a negative value of -0.24 °C, showing a rather high thermal conductivity discussed above. In addition, there might be some ice in the AL that has a higher conduction in the frozen state in winter than in summer when it melts to water.

5.1.2 EN-B-2, moist location

The thermal regime for the borehole in Endalen was calculated for the period 28/09/2008-27/09/2009. MAGST during this period was -0.58 °C. Based on linear interpolation, ALT was estimated at 1.28 m depth, with corresponding TTOP of -3.6 °C.

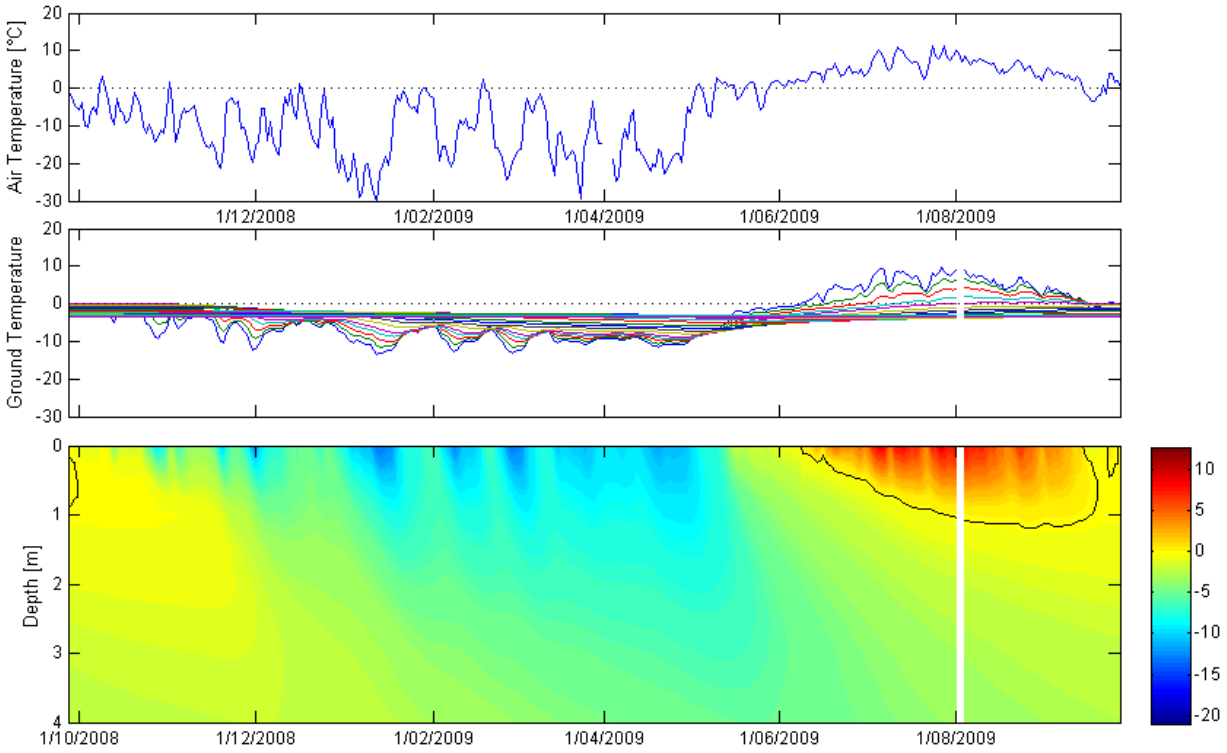

Figure 13 Thermal regime at the wet, continental site of EN-B-1. The uppermost plot represents the annual cycle of the air temperature, in the middle the ground thermal regime at the different sensors is represented with their linearly interpolated temperatures at the bottom. The black line indicates the 0-isotherme, the white stripes indicate data gaps due to instrumental failures.

The thermal regime of this borehole displayed in Figure 13 is comparable to AS-B-2 that is described above. We assume that they share the same meteorology. However, it is important to keep in mind that this site is protected from strong wind action and therefore the accumulation of snow is enabled. Although, the insulating effect of the snow seems to influence the ground temperatures throughout the cold season, there is still a high correlation between GST and AT (e.g. Figure 14). This raises the possibility that the thermal conductivity of the snow-pack that accumulated here is rather high.

The snowmelt is completed at the beginning of June, which corresponds with the time when the thaw progression sets in.

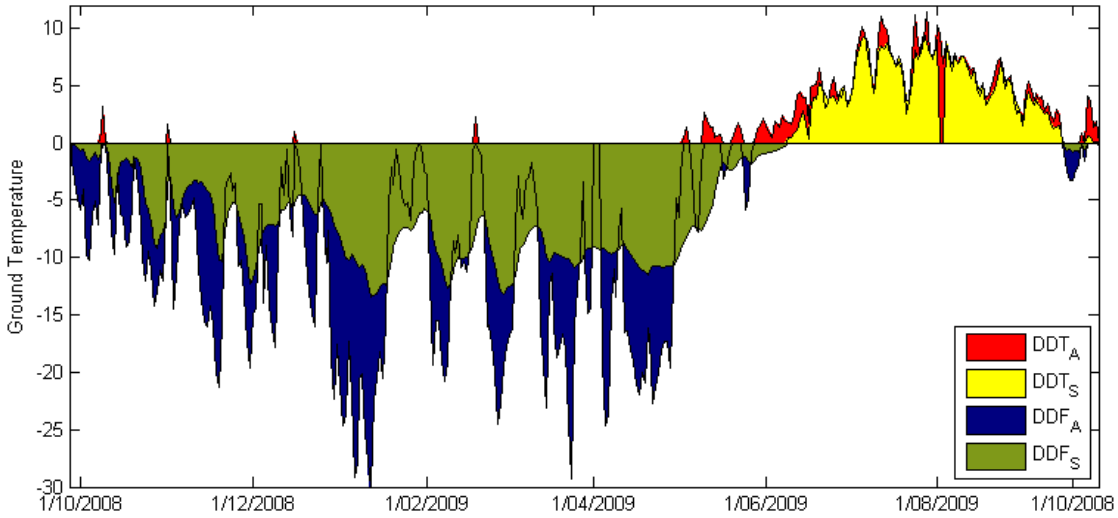

Figure 14 Degree-days of the air and of the ground surface at EN-B-1 illustrate the relation between AT and GST. DDTa and DDTs indicate the thawing degree-days of the air and of the soil respectively; DDFa and DDFs indicate the freezing degree-days of the air and of the soil respectively.

Summer GST follows the air temperatures fluctuations but with slightly less pronounced peaks, probably due to the vegetation buffering effect. AL-thawing proceeds rapidly and to a greater depth than in Adventdalen. This is interesting to note, since the AL thawing starts later at Endalen and the vegetation cover is much more sparse at the Adventdalen site. These findings suggest that other factors influence the ALT apart from the timing of the snowmelt and vegetation effects. The insulation by snow cover is certainly important since it leads to warmer mean ground temperatures, which on the other hand enhance the summer thawing.

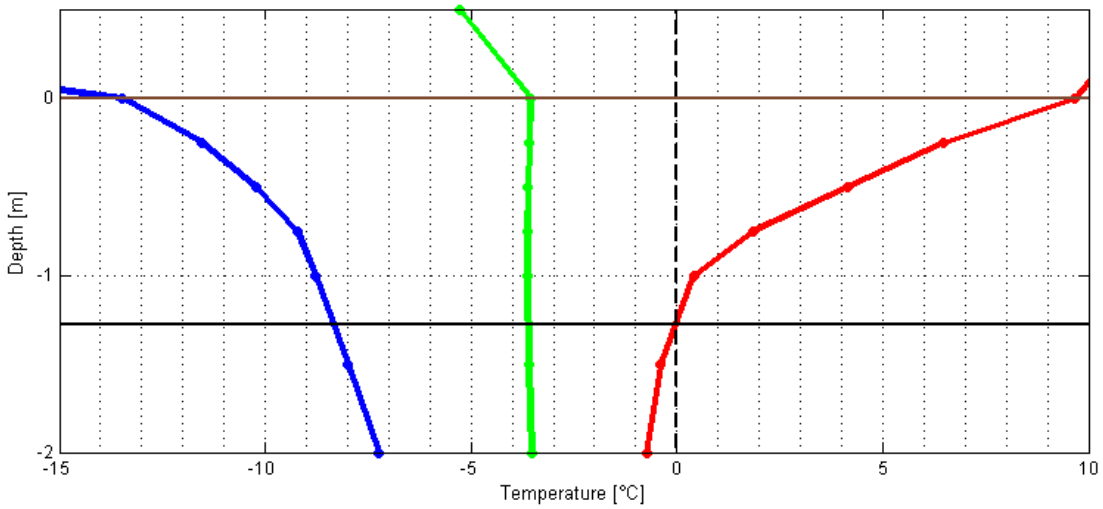

Figure 15 Minimum (blue), average (green) and maximum (red) thermal regime during the analyzed period of 2008-2009 at the EN-B-1 site. The black solid line indicates the ALT; the solid brown line indicates the ground surface; the solid dots indicate the depth at which the sensors are placed.

In addition, it is possible that high ice/water content in the soil plays an important role, leading to rather high heat transfer by conduction, which results in a relatively high thermal offset of -0.03 °C.

The mean surface offset at this site was calculated as 1.72 °C, which represents the highest value of all study sites (see Figure 15). The relatively warm MAGST is probably caused by the above-mentioned insulation effect from the cold winter AT, whereas the cooling effect of the vegetation in summer seems to play a less important role because the warm period of the year is much shorter than the cold period.

5.2 Maritime site

The calculated MAAT at the maritime site during the period analyzed in this work was -3.36 °C. The annual cycle of air temperature at the maritime locality ranged from -21 °C to +12 °C and thus indicates less pronounced amplitude than what has been observed at the continental site, refer to Figure 25 in appendix. Temperatures above 0 °C during the cold period seem to be even more pronounced than in Adventdalen.

5.2.1 KL-B-2, dry location

The thermal regime for the borehole at the dry site of Kapp Linnè was calculated for the period 28/09/2008-27/09/2009. MAGST during this period was -3.70 °C. Based on linear interpolation, ALT was estimated at 1.87 m depth, which is the greatest value of all boreholes and corresponds to the warmest TTOP of -3.11 °C.

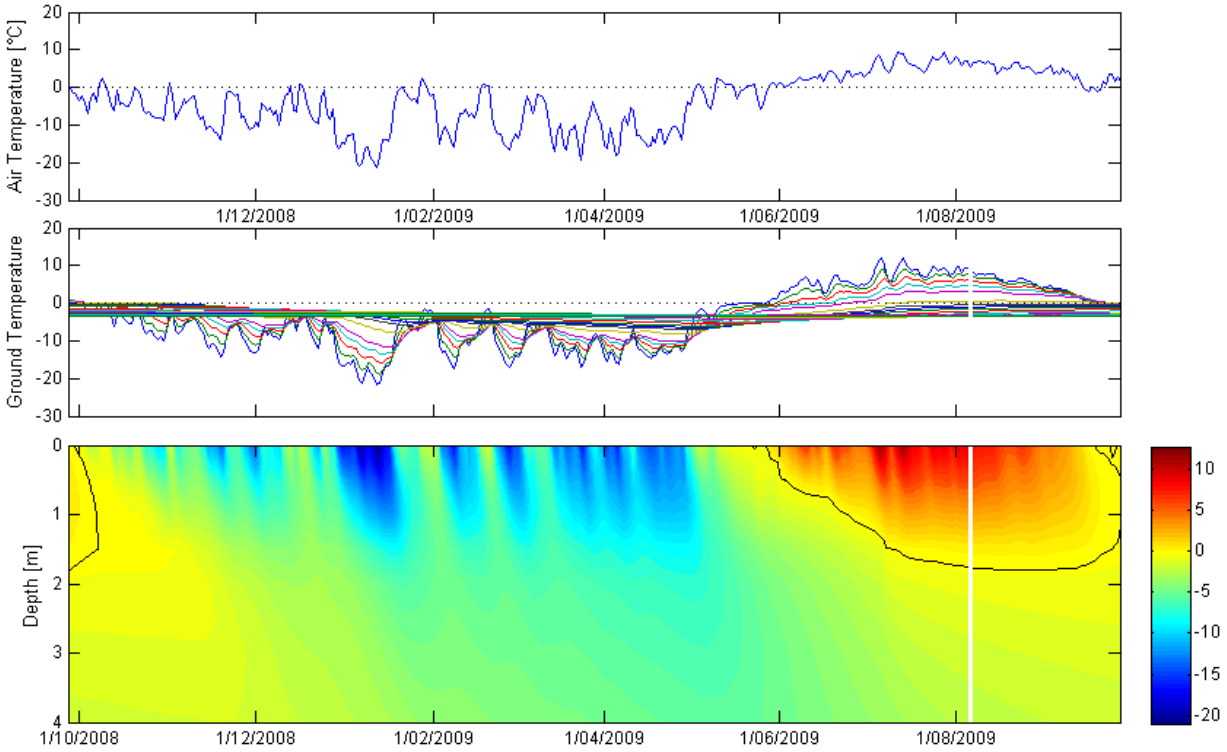

Figure 16 Thermal regime at the dry, maritime site of KL-B-2. The uppermost plot represents the annual cycle of the air temperature, in the middle the ground thermal regime at the different sensors is represented with their linearly interpolated temperatures at the bottom. The black line indicates the 0-isotherme; the white stripes indicate data gaps due to instrumental failures.

Ground thawing sets in at the end of May, with a rapid thaw progression until the freeze-back starts in the end of September and is not completed until the end of the observed period, as observed in Figure 16.

The slow rate of freeze-back at KL-B-2 is probably due to evacuation of latent heat during freezing of thick active layer. Here a small change in temperature seems to require considerable exchange of latent heat due to a possible high unfrozen water content. This

phenomenon has already been found to be characteristic for the delta sediments of the Mackanzie Delta (Kanigan et al., 2009).

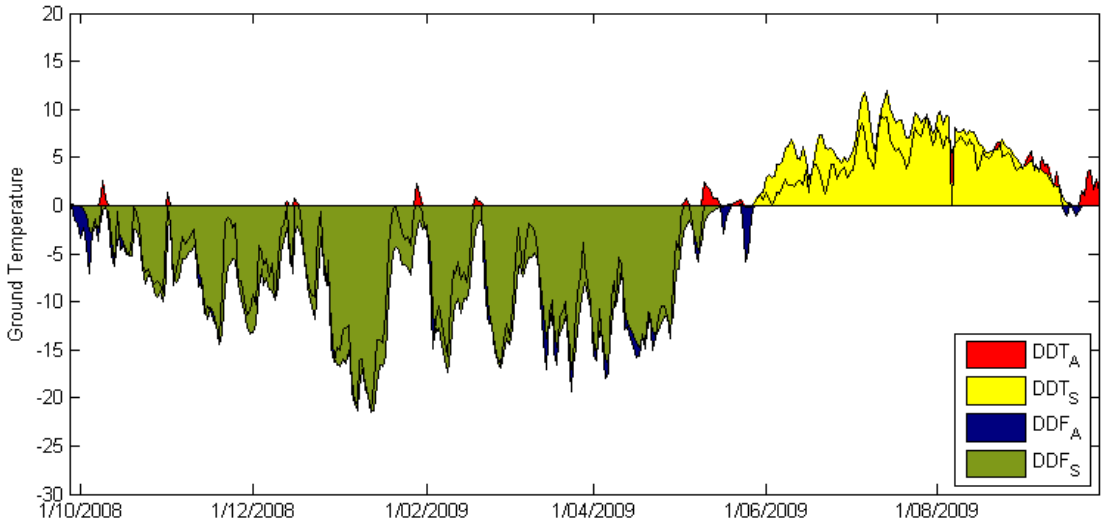

Figure 17 Degree-days of the air and of the ground surface at KL-B-2 illustrate the relation between AT and GST. DDTa and DDTs indicate the thawing degree-days of the air and of the soil respectively; DDFa and DDFs indicate the freezing degree-days of the air and of the soil respectively.

The thermal regime of the borehole shows a very high correlation between GST and AT (e.g. Figure 17). The ground surface temperatures during the cold period, however, indicate slightly lower values than AT during the cold period and somewhat higher values during the warm period. This phenomenon might be caused by the coarse surface material that allows free air convection. In addition, the location of this borehole on a raised beach ridge is prone to strong wind action and snow cover is mostly absent in winter; further, we observed a layer of ice covering the surface, as fieldwork was performed in this area in April 2009. The high thermal conductivity of ice might enhance the penetration of cold temperatures in winter. Whereas there is no vegetation cover that provides any buffering effect to the air temperatures in summer.

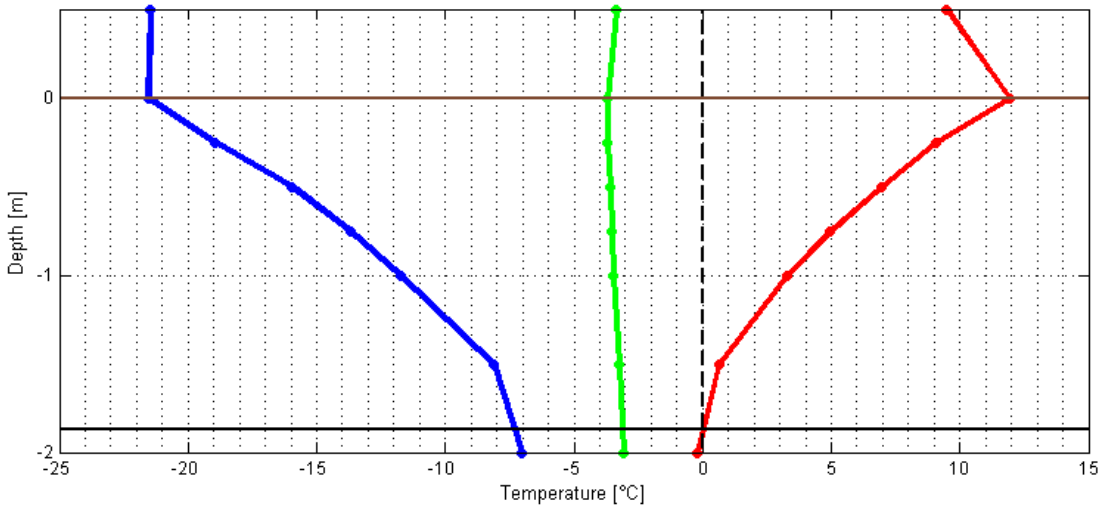

Figure 18 Minimum (blue), average (green) and maximum (red) thermal regime during the analyzed period of 2008-2009 at the KL-B-2 site. The black solid line indicates the ALT; the solid brown line indicates the ground surface; the solid dots indicate the depth at which the sensors are placed.

The surface offset at this site resulted in a negative value of -0.34 °C, while the thermal offset was calculated as 0.59 °C. The positive value of the thermal regime is an uncommon pattern, as stated previously in the background section, MGST are usually lower than TTOP. The phenomena detected at this site might be explained by the absence of snow and vegetation cover resulting in very high air conduction at the upper layer of the AL, with significant cooling of the upper layer of the active layer in winter.

5.2.2 KL-B-3, wet location

The thermal regime for the borehole at the moist site of Kapp Linnè was calculated for the period 28/09/2008-27/09/2009. MAGST during this period was -2.74 °C. Based on linear interpolation, ALT was estimated at 0.83 m depth, corresponding to TTOP of -3.71 °C.

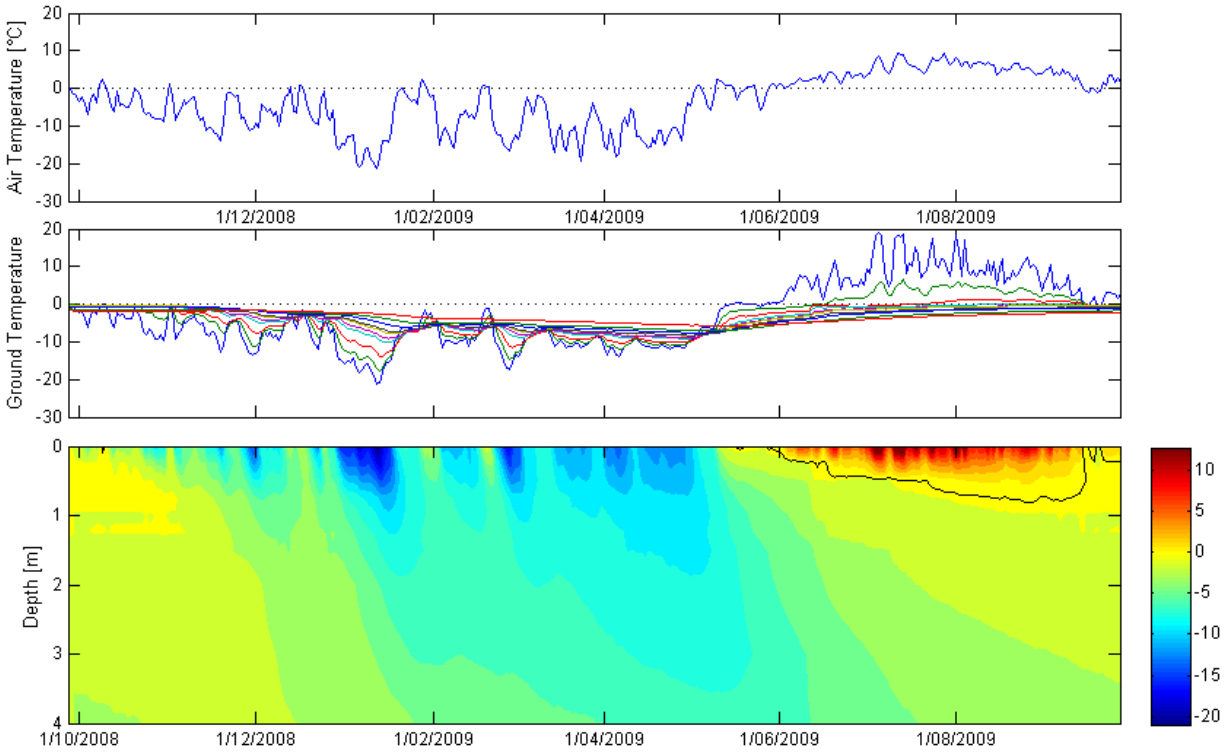

Figure 19 Thermal regime at the wet, maritime site of KL-B-3. The uppermost plot represents the annual cycle of the air temperature, in the middle the ground thermal regime at the different sensors is represented with their linearly interpolated temperatures at the bottom. The black line indicates the 0-isotherme; the white stripes indicate data gaps due to instrumental failures.

Ground thawing set in at the end of May, which represents the same timing as at the nearby dry site of KL-B-2. However, the thaw progression of the AL is much slower and does not reach one meter depth. Obviously the peat layer found at this site plays an important role. In addition, we know that this bog area was wet at the beginning of the warm period and dried out later on. In fact, field investigations revealed the surface was already at the beginning of August 2009. Consequently, the dried organic matter with its low thermal conductivity, together with the vegetation cover at this site, might prevent the ground from forming a deep active layer (see Figure 19).

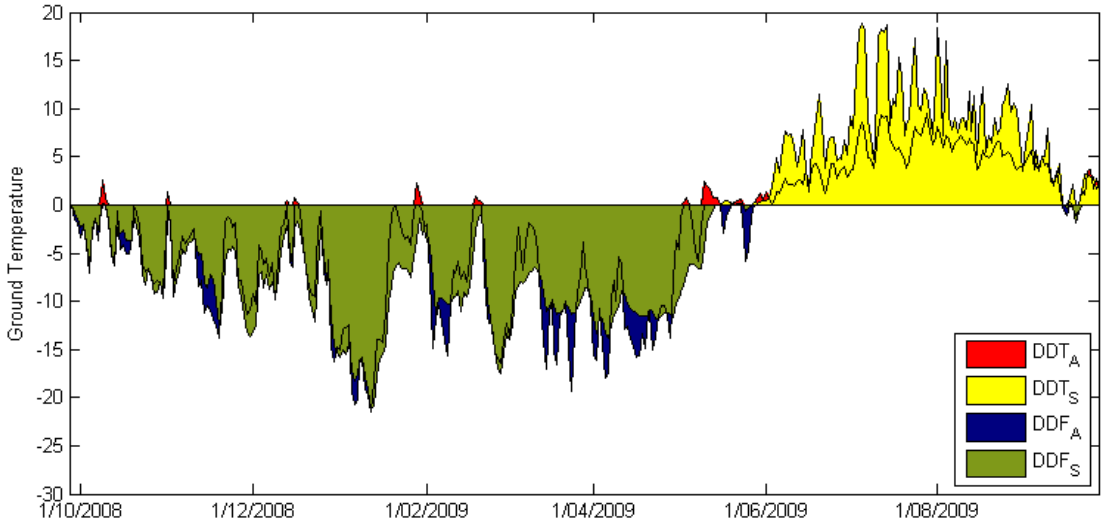

Figure 20 Degree-days of the air and of the ground surface at KL-B-3 illustrate the relation between AT and GST. DDTa and DDTs indicate the thawing degree-days of the air and of the soil respectively; DDFa and DDFs indicate the freezing degree-days of the air and of the soil respectively.

The thermal regime of the borehole shows high correlation between GST and AT. The ground surface temperatures during the cold period, however, presents phases with damped temperatures, probably as a consequence of an insulating snow pack, especially in March and April 2009. But also during these phases there are days with very high correlation between GST and AT, that can be explained by the removal of snow caused by strong wind action or possibly by rain, as liquid precipitation is not uncommon in winter at this maritime location. On the other hand, it is possible that simple melting can also explain the absence of snow during the days with warm air temperatures.

The abnormally high GST during the warm period represented in Figure 20 can be explained with the phenomenon already described for the borehole in Adventdalen, that is to say, the heating effect of the casing tube by sunshine, since the top of the tube with the enclosed data logger reaches above the surface.

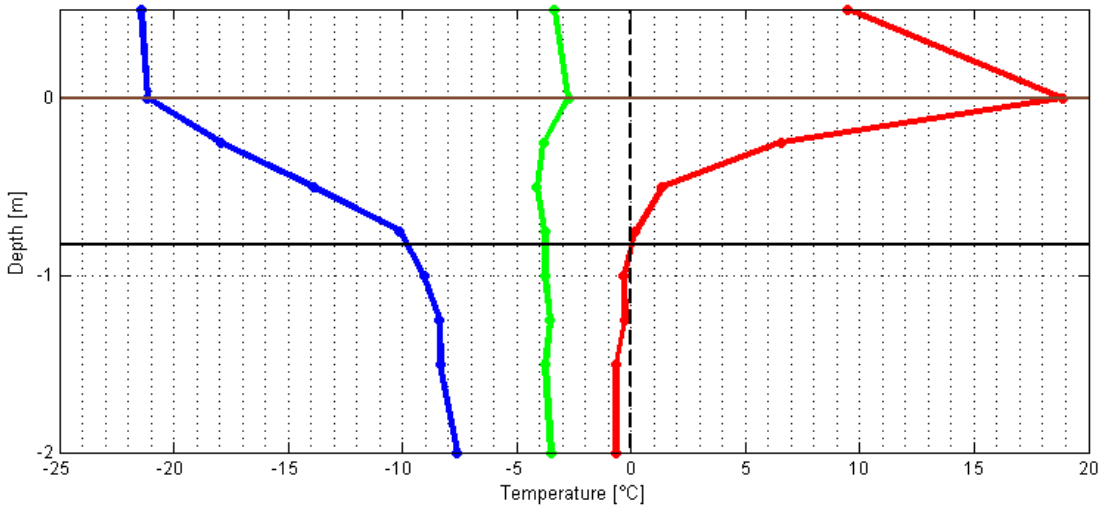

Figure 21 Minimum (blue), average (green) and maximum (red) thermal regime during the analyzed period of 2008-2009 at the KL-B-3 site. The black solid line indicates the ALT; the solid brown line indicates the ground surface; the solid dots indicate the depth at which the sensors are placed.

The temperature difference between MAGST and MAAT at this site was calculated as 0.61 °C. This surface offset might be slightly too high, because of the heating of the casing tube, as described above. The value, however, might indicates a significant cooling effect of the vegetation and a slight damping effect of the snow cover.
The thermal offset was calculated as -0.96 °C, which also has to be considered carefully due to the abnormally high GST, which is visible in the Figure 21. The thermal properties of the organic soil and the presumably high ice/water content might play an important role in the rate of heat transfer by conduction at this site.

Table 5 and 7 give an overview of the calculated standard parameters and of the mean annual average temperatures for the different sensor depths at the four boreholes. Figure 22 illustrates the trumpet curves with the annual thermal cycle for each borehole. These tables and figures make a regional comparison between the maritime influenced Kapp Linnè site and the continental Adventdalen and Endalen boreholes. Further, it is possible to differentiate between the thermal state of permafrost on the local scale by analyzing Figure 24.

Table 5 Overview table of the calculated parameters at the four study sites.

	AS-B-2	**EN-B-1**	**KL-B-2**	**KL-B-3**
MAAT (°C)	-5.24	-5.29	-3.36	-3.36
MAGST (°C)	-4.46	-3.58	-3.70	-2.74
ALT (m)	0.94	1.28	1.87	0.83
TTOP (°C)	-4.75	-3.60	-3.11	-3.71
Surface offset	0.78	1.72	-0.34	0.61
Thermal offset	-0.24	-0.03	0.59	-0.96
Veg. offset	-0.69	0.33	-0.34	-1.01
Nival offset	0.10	2.02	-0.67	-0.40
n_t	1.40	0.80	1.22	1.68
n_f	0.99	0.71	1.14	1.08
DDTair (°C days)	625	611	548	548
DDTsurface (°C days)	877	491	671	918
DDFair (°C days)	2522	2526	1773	1773
DDFsoil (°C days)	2486	1788	2017	1919

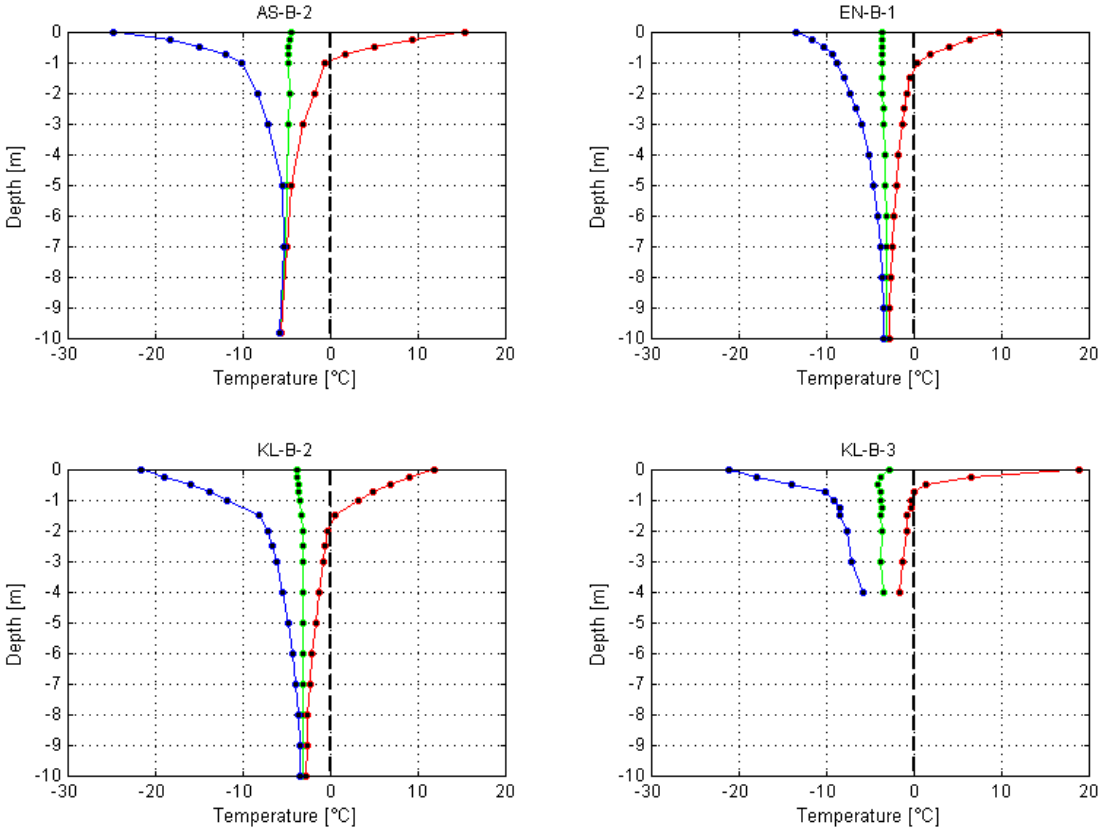

Figure 22 Minimum (blue), average (green) and maximum (red) annual thermal cycles at the four study sites. The black dots indicate the depth at which the sensors are placed. More detailed plots are given in figure 30-34.

5.3 Regional comparison: maritime vs. continental site

The climatic differences between the maritime and the continental site are evident when analyzing the degree-days of the air. DDTa and DDFa are respectively 11% and 42% higher at the continental site (see Table 5). This evidences the significant difference in air temperatures at a regional scale, in particular during the cold period of the year. The tendency for a more continental climate in Adventdalen during winter than during summer may be explained by the proximity of the weather stations to Adventfjorden, which usually is frozen during winter, also documented by Førland et al. (2009b).

Figure 22 shows that permafrost terrains with maritime exposure are underlain by warmer average permafrost temperatures with deeper active layer amplitude depths. KL-B-3, however, has relatively cold permafrost temperatures.

The amplitude of the annual cycle is largest at the AS-B-2 borehole with 40 °C. In fact this amplitude is related to the degree of climate continentality as long as the site-specific factors do not have a considerable influence on the GST. This influence can be seen on the trumpet curve of EN-B-1 that is 13 °C lower than the near-by AS-B-2.

The zero annual amplitude was calculated as 9, 15 and 17 m depth for AS-B-2, EN-B-2 and KL-B-2 respectively. KL-B-3 could not be calculated because the borehole instrumentation only reaches down to 4-m-depth, which is above the ZAA at this site. It is interesting to note that the continental-wet and the maritime-dry study sites show similar ZAA depths.

We can see on these graphs that the permafrost temperatures are highest at KL-B-2 and represent temperatures an average of 1.5 °C higher at the maritime site than at the continental site. The mean annual ground temperatures measured at 0.5-m depth between September 2008 and September 2009 was highest at the KL-B-2 site. A similar pattern was observed at 1-m depth (e.g. Figure 28 and 29).

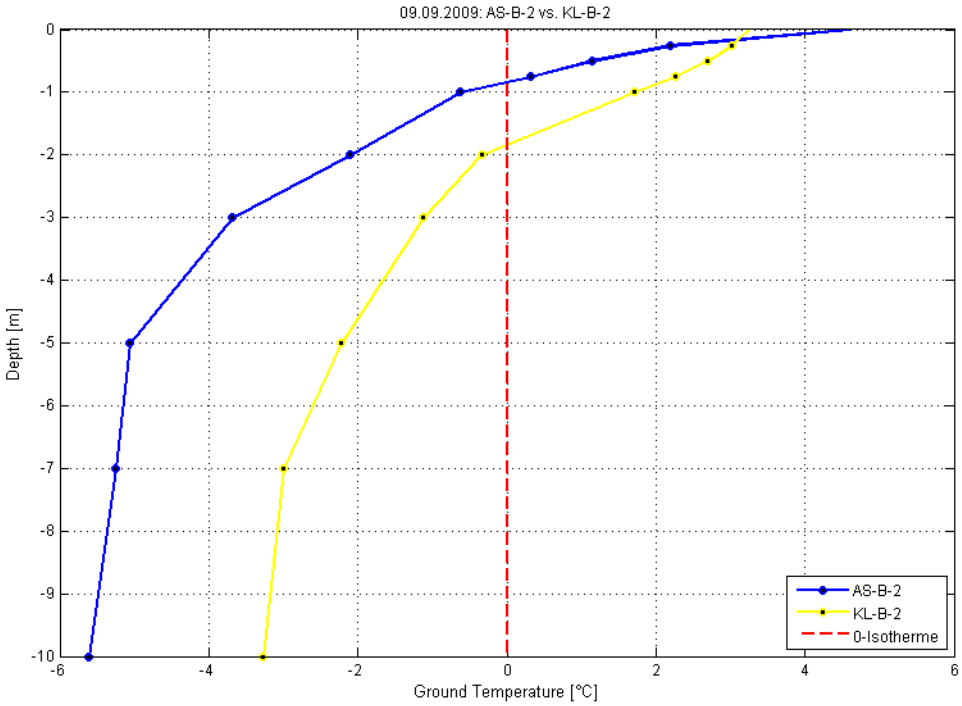

Figure 23 Ground temperatures on the 9th of September 2009 at the two dry locations: AS-B-2 (blue) and KL-B-2 (yellow).

Further evidence of the thermal difference in the dry soils of AS-B-2 an KL-B-2 are represented in Figure 23, where the ground temperatures are plotted against depth on one particular day. A considerable offset is visible between the two locations, with its maximum around 5 m depth. The active layer reaches its maximum around the analyzed date of the above described figure; ALT is roughly double as thick in Kapp Linnè as in Adventdalen. A comparison of thermal differences at the wet sites is given in Figure 34.

5.4 Local comparison: dry vs. wet ground

Differences between the dry and the wet locations are evidenced when comparing the degree-days of the soil. DDTs and DDFs are respectively 78% and 39% higher at the dry continental site relative to the wet continental site. The significant differences evidence the importance of the site-specific factors, such as snow pack at EN-B-1. This is also confirmed by the nf-factor and by the nival offset listed in Table 5. Uneven snow

distribution is important for its insulating effect during autumn and winter. Whereas in spring and summer, snow accumulation leads to large local variation in moisture during the melting season and determines how long the surface remains free of snow.

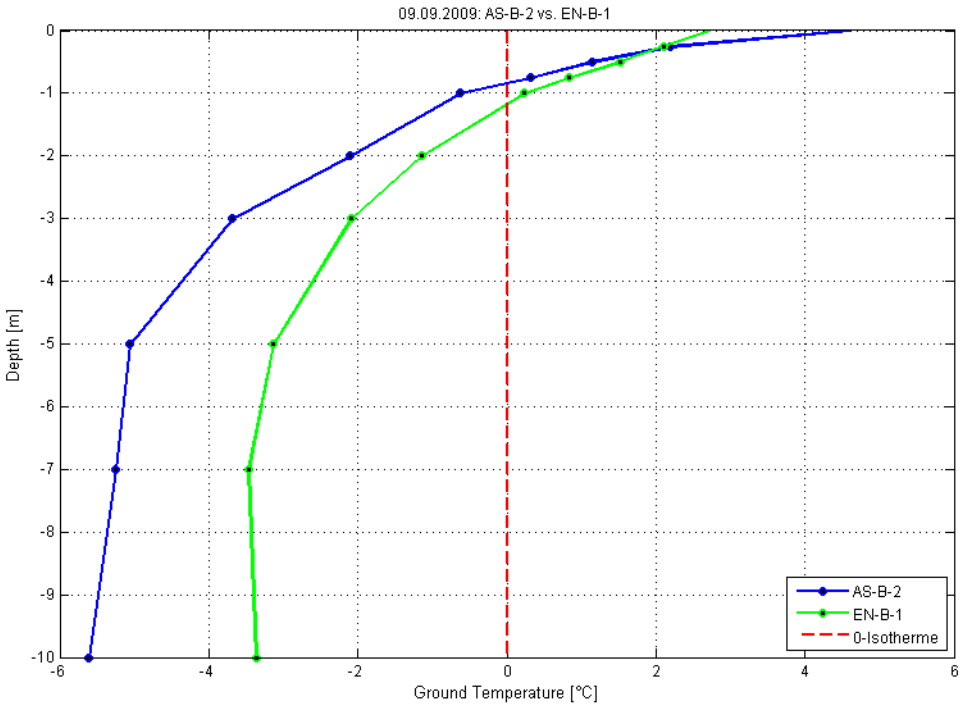

Figure 24 Ground temperatures on the 9th of September 2009 at the two continental locations: AS-B-2 (blue) and EN-B-1 (green).

Figure 24 shows that ground temperatures are significantly higher at EN-B-1 than at the near-by AS-B-2 study site, where the cold winter air temperatures can penetrate into the soil without the insulation effect of a significant snow pack. This is in accordance with the values for freezing degree-days of the ground surface and of the air as seen in Figure 27, which shows a much lower correlation between AT and GST at the EN-B-1 site compared to the AS-B-2 site. The delayed beginning of the thawing period at the EN-B-1 site indicates a prolonged covering of snow. This is further evidence for substantial snow cover effect on thawing progression, whereas air temperatures seem to only have an indirect impact.

The Vegetation cover, on the other hand was parameterized with the nt factor and the vegetation offset, seems to be most relevant at EN-B-1 (e.g. Table 5). Vaganov et al.(2000) have shown that vegetation affects the radiant and convective heat transfer between the air and the underlying inorganic surface and thus the relationship between air temperatures and temperatures at the ground surface. Dry mosses and lichens, especially, can provide a significant insulating value.

DDTs and DDFs at the maritime site were calculated as -27% and 5% for the dry site relative to the wet site. We shall not consider the first result because of the instrumental failure mentioned previously. Whereas the 5% difference during the cold period supports the theory of a shallow snow pack covering KL-B-3, during March and April, as seen in Figure 20. The buffering effect by snow is further defined through the slightly higher value of the vegetation offset and the lower value of nf relative to the dry maritime site.

It is interesting to note that permafrost temperatures are colder under the soil rich in peat than in the adjacent areas of the raised beach ridge (e.g. Table 7). The influence of organic layer on ground thermal conditions has been well documented by Nakano and Brown (1972). Figure 35 shows the thermal difference of the maritime sites on the 9th of September 2009.

6 Discussion

The purpose of this study was to compare the thermal state of permafrost at different locations in Spitsbergen. We approached the question of whether or not significant ground temperature differences exist at a regional and at a local scale in central and western Spitsbergen during the hydrological year of 2008-2009. Such variations in thermal regimes were then related to the influence of meteorology, mainly air temperatures and precipitation, and the effect of site-specific parameters, such as

vegetations, snow cover and lithology. The aim of this work was to understand the relation between meteorology, site-specific factors and ground temperatures in Spitsbergen in order to evaluate the possible impact of climate change on permafrost at this High Arctic region.

Values of mean annual air temperatures during the analyzed period were 1.8 °C lower at the continental site of Adventdalen that at the more maritime influence site of Kapp Linnè. Moreover, the values for 2008-2009 differed considerably from the normal values. As stated previously, MAAT was -6.7 °C for the Longyearbyen area during the period 1975-1990, while it was calculated as -5.2 °C for the herewith analyzed hydrological year. MAAT at Kapp Linnè was -5.1 °C during the period 1961-1990 and it was only -3.4 °C during the period 2008-2009.

The regional difference in meteorology plays an important role in determining ground temperatures at the analyzed boreholes. Yet, air temperatures alone do not account for variations in the subsurface temperatures. In fact, as stated by (Williams and Smith, 1989) it is rare that any single factor alone can explain local ground thermal conditions. The ground thermal regime results from the interaction of climatic, surface and subsurface factors, and this is ultimately responsible for the variations in ground temperatures which occur locally.
For instance the interplay between the considerable snow cover and the thermal conductivity expressed by the thermal offset seems to be largely responsible for the warmer ground temperature at the EN-B-1 location.

Nevertheless, we had difficulties interpreting the precise effect of snow cover at the analyzed study sites. There is no measuring system to determine the exact snow thickness and the thermal conductivity of the snow pack, which can vary greatly due, for instance, to the wind action. Further limitations were set by the missing data of ice content in the permafrost at all study sites. Ice determines to a great extent the high thermal conductive properties of frozen soil, for example at the wet locations.

Vegetation cover, another local environmental variable, does not seem to play a significant role at the analyzed study sties. The buffering effect of plant cover is only visible at the EN-B-2 site with the according low nt-factor. Essentially, the sparse vegetation makes the barren surfaces of the High Arctic highly susceptible to climate change. Such terrains are classified by Shur and Jorgensen (2007) as climate-driven permafrost. This type of permafrost is perhaps the most vulnerable type of permafrost to the rapid climate warming expected in the next few centuries because warming is likely to occur at a faster rate than ecological succession.

Features of the annual cycle illustrate the active layer amplitude depth with shallowest seasonal frost at the dry continental site in Adventdalen. This site is meant to be highly susceptible to meteorological variations, in particular to air temperatures as stated by Chrisitansen and Humlum (2008). A more detailed and long-term monitoring of active layer thickness and top permafrost thermal state has been ongoing since the year 2000 at the UNISCALM site, on the same loess-covered terrace as the AS-B-2 borehole is situated. According to the above-cited authors, MAAT at this site varied between -1.7 °C and -6.1 °C since 2000. This is an indication for the significant interannual variations of air temperatures and thus of the ground temperatures recorded at this site. Accordingly, the year 2008-2009 was rather cold, which has to be taken into consideration for the analysis of this thesis.

Ground temperatures recorded at the top of the permafrost are highly variable from site to site. Relatively warm permafrost temperatures were detected at the beach ridge site in Kapp Linnè and at the solifluction station in Endalen. Lunardini (1996) announced the sensitivity of warm permafrost emphasizing the ultimate limiting condition for permafrost occurrence when TTOP equals 0 °C.

The changing meteorological conditions in the Polar Regions, in particular those described by (Førland et al., 2009b) for the Svalbard archipelago, may cause higher snow accumulations, which can lead to warmer permafrost temperatures, as seen from the wet-

continental site in Endalen. In fact, the timing and the amount of snowfall seem to play a crucial role in determining ground temperatures in central and western Spitsbergen.

Results from the PACE borehole sites indicate that the permafrost terrains have been exposed to atmospheric warming in all seasons since 1975, as stated in Harris et al. (2009). The warming has been especially pronounced during the autumn and winter for the northernmost boreholes, especially the one located on Svalbard, near Adventdalen with its near surface warming of 1-2 °C over the last 6-8 decades (Isaksen et al., 2000; Isaksen et al., 2007). These first results also support the presumption that snow thickness and duration strongly modulate the response of near-surface permafrost temperatures to changes in air temperature.

7 Conclusion and perspectives

The annual cycles of soil and air temperatures as well as the field observations of snow and vegetations cover lead to the following five general conclusions:

1) Low surface offset and direct atmosphere-ground coupling especially in summer characterizes the barren surfaces with little or no vegetation at the four study sites in central and western Spitsbergen.

2) Natural variations in microclimatic and terrain conditions introduce significant variations to the surface temperatures regime within even a small area. The effect of varying snow cover seems to play the most important role, while the impact of vegetation is almost negligible.

3) Seasonal ground thermal fluctuations within the zero annual amplitude are determined to a great extent by local environmental variables whereas long-term climatic variations influence frozen ground to greater depths with considerable time-lags.

4) Climate change may affect primarily the warm permafrost sites, which are represented in this work by the dry, maritime site in Kapp Linnè and by the wet, continental site in Endalen.

5) Nevertheless, changing precipitation patterns, in particular the timing and the amount of snowfall as well as the distribution and the conductivity of the snow pack, may play a crucial roles in future ground temperature changes.

The analyses of the thermal state of permafrost at the four study sites presented above underscore the need for multi-annual time series and for a larger framework of examined parameters to understand the regional differences in the ground thermal regime. In fact, there are several influencing factors that determine the meteorological influence on permafrost in addition to air temperature. Precipitation in liquid and in solid form, cloud cover and type, wind direction and speed, for instance, should be taken into consideration. Further, it is important to dispose of precise conductivity values determined to a great extent by the ice/water content of the soil. Thus this study cannot be presented as conclusive. Nevertheless, taking into consideration the limited amount of parameters that could be analyzed due to the reduced extensiveness of this thesis, this study gives a broad overview of different thermal states that exist within lowland permafrost areas in the High Arctic.

Acknowledgments

The fieldwork has been financially supported by the University Centre of Svalbard (UNIS), the Graduate School of Climate Sciences, Bern and the HBM foundation, Basel. My supervisors were Prof. Christian Schlüchter, Prof. Hanne Christiansen and PD Dr. Frank Preusser, who provided support during the internship and during the writing of the thesis. I greatly appreciate the encouragement from several people at UNIS and at the University of Bern, Ullrich Neumann for helping with fieldwork, Håvard Juliussen for supporting me when starting to write the thesis, Ruben Van De Kerchove and Dimitri Meier for their precious help with Matlab and especially Frank Preusser for leading me to the fascinating High Arctic environment of Svalbard.

References

ACIA, 2005: *Arctic Climate Impact Assessment*. New York, Cambridge University Press, (Symon, C., Arris, L., and Heal, B. (eds.)), 1042 pp.

Åkerman, J., 1980: *Studies on periglacial geomorphology in West Spitsbergen*. Lund: Lunds universitet, 297 pp.

André, M. F., 1994: Rock glaciers in Svalbard: tentative dating and inferred long-term velocities. *Geografiska annaler. Series A. Physical geography,* 76: 235-245.

André, M. F., 1997: Holocene rockwall retreat in Svalbard: a triple-rate evolution. *Earth Surface Processes and Landforms,* 22: 423-440.

Anisimov, O., Shiklomanov, N., and Nelson, F., 2002: Variability of seasonal thaw depth in permafrost regions: a stochastic modeling approach. *Ecological Modelling,* 153: 217-227.

Brown, R., Evan, R., Research, N. R. C. C. D. o. B., and Péwé, T., 1973: *Distribution of permafrost in North America and its relationship to the environment: a review, 1963-1973*: 1973.

Bruland, O., Marechal, D., Sand, K., and Killingtveit, Å., 2001: Energy and water balance studies of a snow cover during snowmelt period at a high arctic site. *Theoretical and Applied Climatology,* 70: 53-63.

Chapin, F. S., Sturm, M., Serreze, M. C., McFadden, J. P., Key, J. R., Lloyd, A. H., McGuire, A. D., Rupp, T. S., Lynch, A. H., and Schimel, J. P., 2005: Role of land-surface changes in Arctic summer warming. *Science,* 310: 657-660.

Christensen, T., Johansson, T., Akerman, H., Mastepanov, M., Malmer, N., Friborg, T., Crill, P., and Svensson, B., 2004: Thawing sub-arctic permafrost: Effects on vegetation and methane emissions. *Geophysical Research Letters,* 31: 1-4.

Christiansen, H. and Humlum, O., 2008: Interannual variations in active layer thickness in Svalbard. *Proceedings Ninth International Conference on Permafrost, June 29-July 3,* 1: 257–262.

Corbel, J., 1966: Datation au C 14 des terrasses marines de la baie du Roi'. *Spitsberg 1964–RCP 42–CNRS*: 309–314.

Dickson, R. R., Osborn, T. J., Hurrell, J. W., Meincke, J., Blindheim, J., Adlandsvik, B., Vinje, T., Alekseev, G., and Maslowski, W., 2000: The Arctic Ocean response to the North Atlantic Oscillation. *Journal of Climate,* 13: 2671-2696.

Førland, E. J., Hanssen-Bauer, I., and Nordli, P., 1997: Climate statistics and longterm series of temperature and precipitation at Svalbard and Jan Mayen. *DNMI report,* 21: 97.

Førland, E. J., Benestad, R. E., Flatøy, F., Hanssen-Bauer, I., Haugen, J. E., Sorteberg, A., and Ådlandsvik, B., 2009: *Climate development in North Norway and the Svalbard region during 1900-2100*. Tromsø, Norsk polarinstitutt (eds.), 43 s. pp.

Forman, S. L. and Miller, G. H., 1984: Time-dependent soil morphologies and pedogenic processes on raised beaches, Bröggerhalvöya, Spitsbergen, Svalbard archipelago. *Arctic and Alpine Research,* 16: 381-394.

French, H. M., 2007: *The periglacial environment*. Chichester: Wiley, 458 pp.

Furrer, G., 1994: Zur Gletschergeschichte des Liefdefjords/NW-Spitsbergen. (On the glacial history of Liefdefjorden, NW Spitsbergen.). *N.F., Suppl. -Bd.*, 97: 43-47.

Hammer, T. A., Ryan, W. L., and Zirjacks, W. L., 1985: Ground temperature observations. *In* Krzewinski, T. G. (ed.), *Thermal design considerations in frozen ground engineering*. New York: ASCE, 8-52.

Hanssen-Bauer, I., Solås, M. K., and Steffensen, E. L., 1990 *The climate of Spitsbergen*. DNMI-Rapport No. 39:90, Klima, Oslo, 40 pp.

Harris, C., Arenson, L. U., Christiansen, H. H., Etzelmüller, B., Frauenfelder, R., Gruber, S., Haeberli, W., Hauck, C., Hölzle, M., and Humlum, O., 2009: Permafrost and climate in Europe: Monitoring and modelling thermal, geomorphological and geotechnical responses. *Earth Science Reviews,* 92: 117-171.

Hinzman, L. D. and Kane, D. L., 1993: Potential Repsonse of an Arctic Watershed During a Period of Global Warming. *Journal of Geophysical Research-Atmospheres*, 97: 2811–2820.

Hjort, C., 1997: Glaciation, climate history, changing marine levels and the evolution of the Northeast Water Polynya. *Journal of Marine Systems,* 10: 23-33.

Houghton, J. T., Ding, Y., Griggs, D. J., Noguer, M., Van der Linden, P. J., Dai, X., Maskell, K., and Johnson, C. A., 2001: *Climate change 2001: The scientific basis.* Cambridge: Cambridge University Press

Hubberten, H. W., Andreev, A., Astakhov, V. I., Demidov, I., Dowdeswell, J. A., Henriksen, M., Hjort, C., Houmark-Nielsen, M., Jakobsson, M., and Kuzmina, S., 2004: The periglacial climate and environment in northern Eurasia during the Last Glaciation. *Quaternary Science Reviews*, 23: 1333-1357.

Humlum, O., Instanes, A., and Sollid, J. L., 2003: Permafrost in Svalbard: a review of research history, climatic background and engineering challenges. *Polar Research*, 22: 191-215.

Humlum, O., Elberling, B., Hormes, A., Fjordheim, K., Hansen, O. H., and Heinemeier, J., 2005: Late-Holocene glacier growth in Svalbard, documented by subglacial relict vegetation and living soil microbes. *The Holocene,* 15: 396-407.

IPCC, 2007: *Climate change 2007: the physical science basis : contribution of Working Group I to the fourth assessment report of the Intergovernmental Panel on Climate Change*. Cambridge, Cambridge University Press, 996 pp.

Isaksen, K., Muhll, D., Gubler, H., Kohl, T., and Sollid, J., 2000: Ground surface-temperature reconstruction based on data from a deep borehole in permafrost at Janssonhaugen, Svalbard. *Annals of Glaciology,* 31: 287-294.

Isaksen, K., Sollid, J., Holmlund, P., and Harris, C., 2007: Recent warming of mountain permafrost in Svalbard and Scandinavia. *Journal of Geophysical Research-Earth Surface*, 112: 1-11.

Ivanova, E. V., Murdmaa, I. O., Duplessy, J. C., and Paterne, M., 2002: Late Weichselian to holocene paleoenvironments in the Barents Sea. *Global and Planetary Change*, 34: 209-218.

Jeppesen, J. W., 2001: Palæoklimatiske indicatorer for central Spitsbergen, Svalbard. Eksemplificeret ved studier af iskiler og deres værtssedimenter, M. Sc. thesis, The University Center in Svalbard (UNIS), Longyearbyen.

Kanigan, J. C. N., Burn, C. R., and Kokelj, S. V., 2009: Ground temperatures in permafrost south of treeline, Mackenzie Delta, Northwest Territories. *Permafrost and Periglacial Processes,* 20: 127-139.

Koç, N., 1993: Paleoceanographic reconstructions of surface ocean conditions in the Greenland, Iceland and Norwegian Seas through the last 14 ka based on diatoms. *Quaternary Science Reviews,* 12: 115-140.

Liestol, O., 1977: Pingos, springs and permafrost. *Norsk Polarinslutt Arbok 1975*: 7-29.

Liestøl, O., 1976: Pingos, springs and permafrost in Spitsbergen. *Norsk Polarinstitutt Arbok,* 1975: 7-29.

Lunardini, V. J., 1978: Theory of n-factors and correlation of data. *Permafrost: Third International Conference, Proceedings*: 40-46.

Lunardini, V. J., 1996: Climatic warming and the degradation of warm permafrost. *Permafrost and Periglacial Processes,* 7: 311-320.

Major, H. and Nagy, J., 1972: *Geology of the Adventdalen map area*: Norsk Polarinstitutt, 58 pp.

Major, H., Dallmann, W. K., Kjærnet, T., Nøttvedt, A., Tolgensbakk, J., Sørbel, L., and Høgvard, K., 2001: *Geomorphological and Quaternary Geological Map of Svalbard 1:100,000*. Tromsø: Norsk polarinstitutt, 78 pp.

Nakano, Y. and Brown, J., 1972: Mathematical modeling and validation of the thermal regimes in tundra soils, Barrow, Alaska. *Arctic and Alpine Research,* 4: 19-38.

Noetzli, J., Hoelzle, M., and Haeberli, W., Mountain permafrost and recent Alpine rock-fall events: a GIS-based approach to determine critical factors, 2: 827–832.

Nordli, P. Ø. and Kohler, J., 2004: *The early 20th century warming: daily observations at Grønfjorden, and Longyearbyen on Spitsbergen*. Oslo, Norwegian Meteorological Institute (eds.), 20 pp.

Oechel, W. C., Vourlitis, G. L., Hastings, S. J., Zulueta, R. C., Hinzman, L., and Kane, D., 2000: Acclimation of ecosystem CO2 exchange in the Alaskan Arctic in response to decadal climate warming. *Nature,* 406: 978-981.

Ohta, Y., Hjelle, A., Andresen, A., Dallmann, W. K., and Salvigsen, O., 1992: Geological Map of Svalbard 1: 100000, Sheet B9g Isfjorden, *Norsk Polarinstitutt Temakart*, 16-52.

Overpeck, J., Hughen, K., Hardy, D., Bradley, R., Case, R., Douglas, M., Finney, B., Gajewski, K., Jacoby, G., and Jennings, A., 1997: Arctic environmental change of the last four centuries. *Science,* 278: 1251-1256.

Rachold, V., Bolshiyanov, D. Y., Grigoriev, M. N., Hubberten, H. W., Junker, R., Kunitsky, V. V., Merker, F., Overduin, P. P., and Schneider, W., 2007: Nearshore Arctic subsea permafrost in transition. *Eos,* 88: 149–156.

Romanovskii, N. N., Hubberten, H. W., Gavrilov, A. V., Eliseeva, A. A., and Tipenko, G. S., 2005: Offshore permafrost and gas hydrate stability zone on the shelf of East Siberian Seas. *Geo-marine letters,* 25: 167-182.

Salvigsen, O., 2002: Radiocarbon-dated Mytilus edulis and Modiolus modiolus from northern Svalbard: climatic implications. *Norsk Geografisk Tidsskrift,* 56: 56-61.

Serreze, M. C., Walsh, J. E., Chapin, F. S., Osterkamp, T., Dyurgerov, M., Romanovsky, V., Oechel, W. C., Morison, J., Zhang, T., and Barry, R. G., 2000: Observational evidence of recent change in the northern high-latitude environment. *Climatic Change,* 46: 159-207.

Shur, Y. and Jorgenson, M., 2007: Patterns of permafrost formation and degradation in relation to climate and ecosystems. *Permafrost and Periglacial Processes,* 18: 7-19.

Smith, M., 1975: Microclimatic influences on ground temperatures and permafrost distribution, Mackenzie Delta, Northwest Territories. *Canadian Journal of Earth Sciences,* 12: 1421-1438.

Smith, M. W. and Riseborough, D. W., 2002: Climate and the limits of permafrost: a zonal analysis. *Permafrost and Periglacial Processes,* 13: 1-15.

Permafrost Subcommittee, 1988: *Glossary of permafrost and related ground-ice terms*. Ottawa, National Research Council of Canada, Associated Committee on Geotechnical Research (eds.).

Svensson, H., 1969: Pingos i yttre delen av Adventdalen. *Norsk Polarinstitutt Årbok*, 1969: 168–174.

Tolgensbakk, J., Sørbel, L., and Høgvard, K., 2000: Adventdalen, geomorphological and quaternary geological map, Svalbard 1: 100,000, Spitsbergen sheet C9Q, *Norsk Polarinstitutt Temakart*.

Vaganov, E., Eugster, W., Rouse, W., Pielke Sr, R., Joseph, P., Mcfadden, D., Baldocchi, T., Kittel, F., Chapin, S., and Glen, E., 2000: Land-atmosphere energy exchange in Arctic tundra and boreal forest: available data and feedbacks to climate. *Global Change Biology*, 6: 84-115.

Waelbroeck, C., 1993: Climate-soil processes in the presence of permafrost: A systems modelling approach. *Ecological Modelling,* 69: 185-225.

Walker, D. A., Epstein, H. E., Romanovsky, V. E., Ping, C. L., Michaelson, G. J., Daanen, R. P., Shur, Y., Peterson, R. A., Krantz, W. B., and Raynolds, M. K., 2008: Arctic patterned-ground ecosystems: A synthesis of field studies and models along a North American Arctic Transect. *Jurnal of Geophysical Research*, 113: 1-17.

Williams, P. J. and Smith, M. W., 1989: *The frozen earth: fundamentals of geocryology*. Cambridge: Cambridge University Press 302 pp.

Appendix

Table 6 List of symbols used in this thesis.

MAAT	Mean Annual Air Temperature
MAGST	Mean Annual Ground Surface Temperature
GST	Ground Surface Temperature
GT	Ground Temperature
AT	Air Temperature
DDFa	Freezing Degree Days of the air
DDTa	Thawing Degree Days of the air
DDFs	Freezing Degree Days of the soil
DDTs	Thawing Degree Days of the soil
P	Period (365 days)
n_t	thawing n-factor
n_f	freezing n-factor

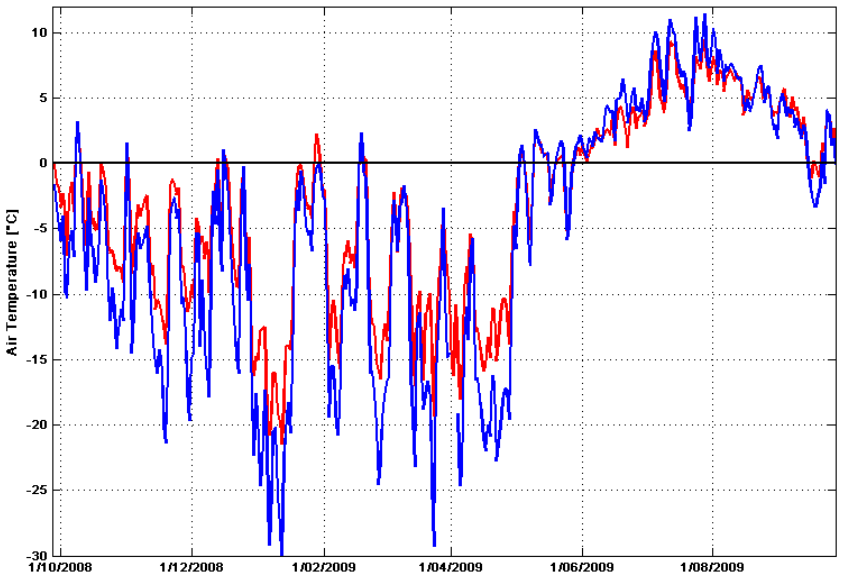

Figure 25 Comparison between the air temperature regimes at the continental (blue) and at the maritime (red) site.

Table 7 Overview table of the mean annual air and ground temperatures at the four study sites.

	AS-B-2 (10)	EN-B-1 (19)	KL-B-2 (23)	KL-B-3 (10)
MAAT	-5.24	-5.29	-3.36	-3.36
MAGST	-4.46	-3.57	-3.70	-2.74
Amplitude at GST	40	23	33	40
-0.25	-4.50	-3.58	-3.70	-3.83
-0.50	-4.69	-3.61	-3.60	-4.11
-0.75	-4.71	-3.65	-3.52	-3.77
-1	-4.77	-3.65	-3.46	-3.78
-2	-4.52	-3.52	-3.07	-3.52
-3	-4.81	-	-3.06	-3.69
-4	-	-3.25	-3.05	-3.05
-5	-4.88	-3.17	-3.04	-
-6	-	-3.10	-3.01	-
-7	-5.09	-3.06	-3.00	-
-8	-	-3.03	-3.01	-
-9	-5.64	-3.03	-3.01	-
-10	-	-3.04	-3.03	-
-12	-	-3.37	-3.06	-
-15	-	-3.19	-3.15	-
-19	-	-3.33	-	-
-20	-	-	-3.28	-
-25	-	-	-3.39	-
-30	-	-	-3.48	-
-35	-	-	-3.53	-
-38	-	-	-3.54	-

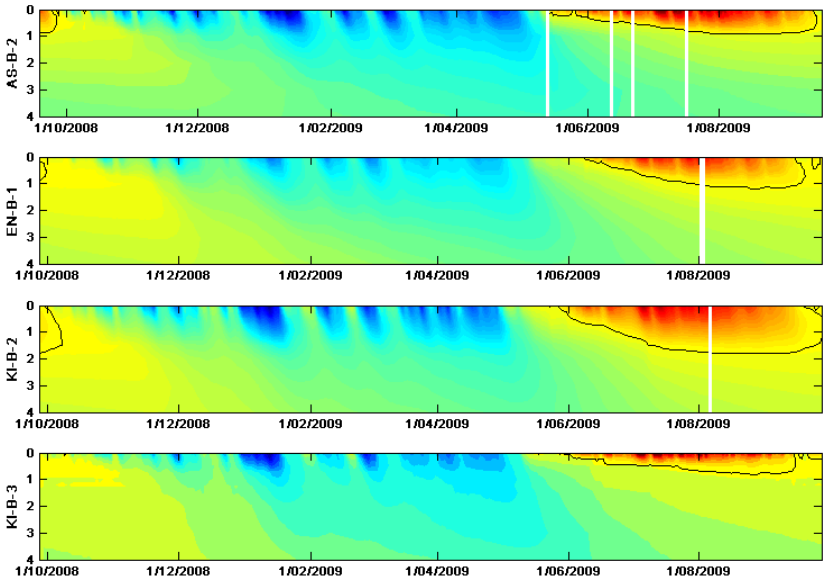

Figure 26 Ensemble of the interpolated ground temperatures at the four study sites.

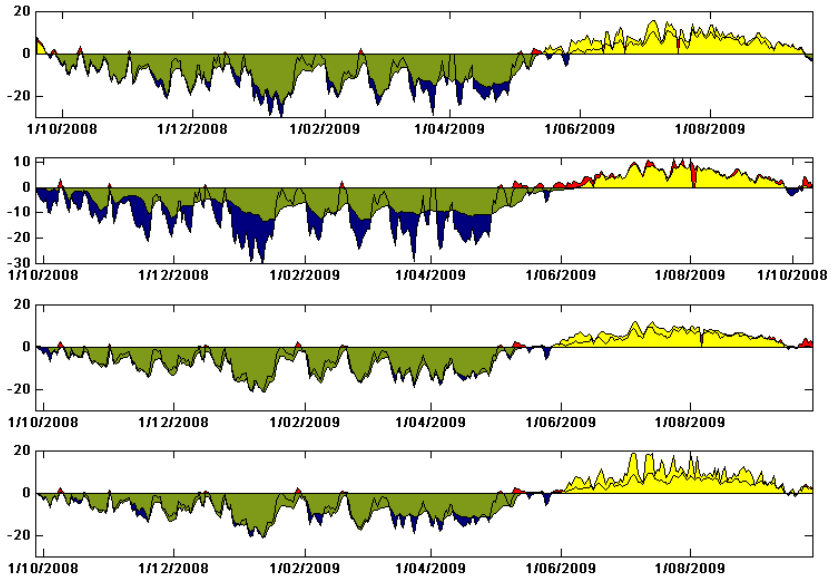

Figure 27 Ensemble of the degree-days at the four study sites.

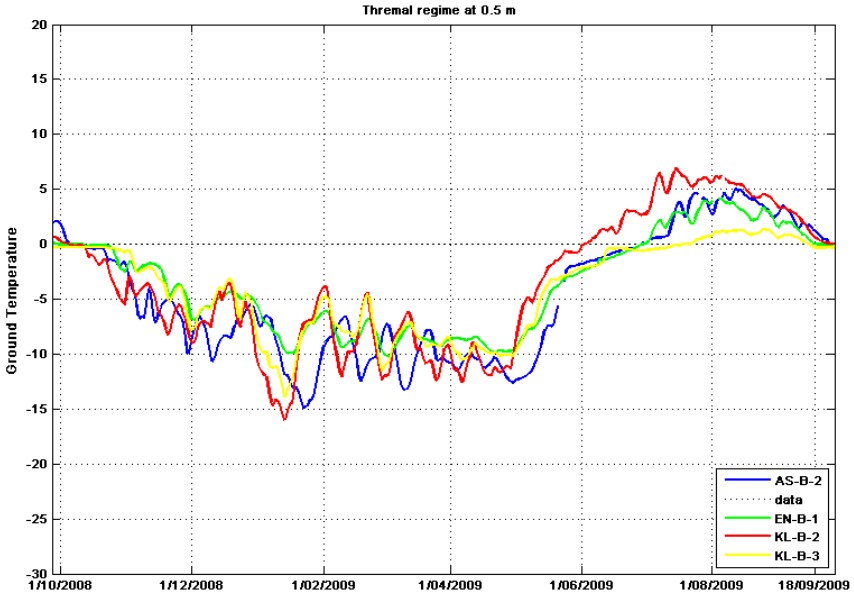

Figure 28 Thermal regime of the -0.5 m sensors at the four study sites.

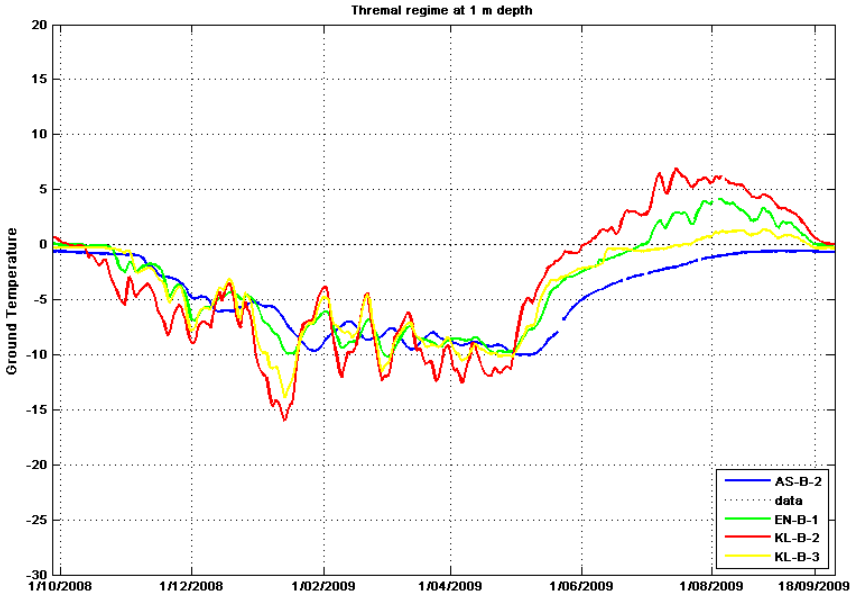

Figure 29 Thermal regime of the -1 m sensors at the four study sites.

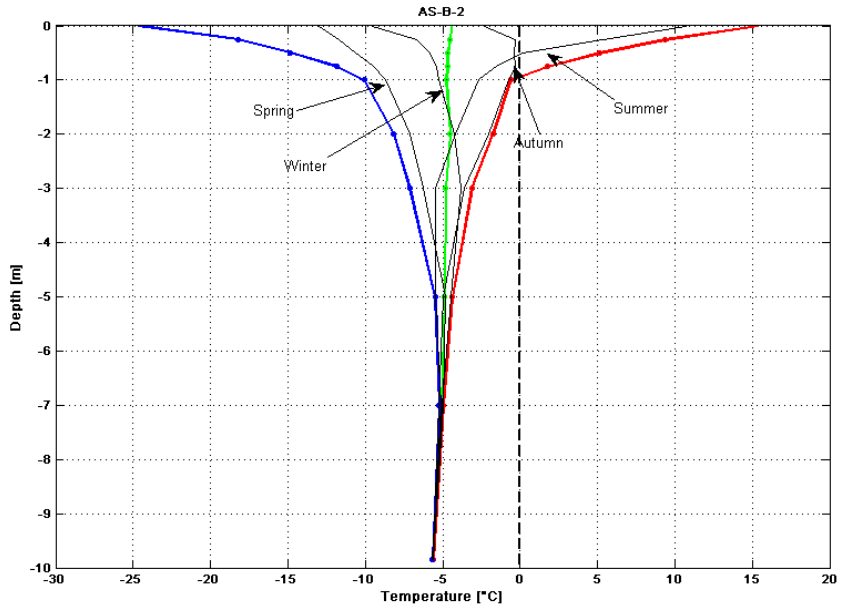

Figure 30 Trumpet curves at the AS-B-2 site.

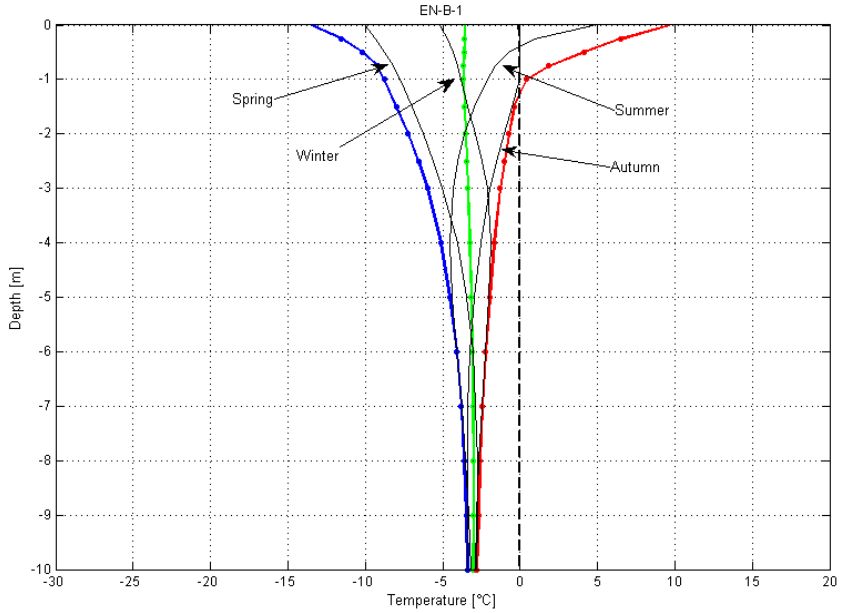

Figure 31 Trumpet curves at the EN-B-1 site.

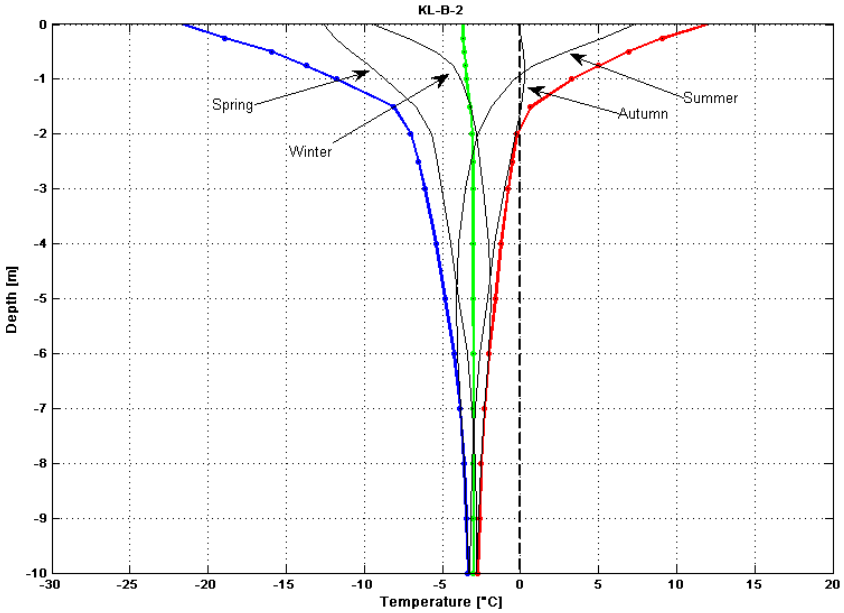

Figure 32 Trumpet curves at the KL-B-2 site.

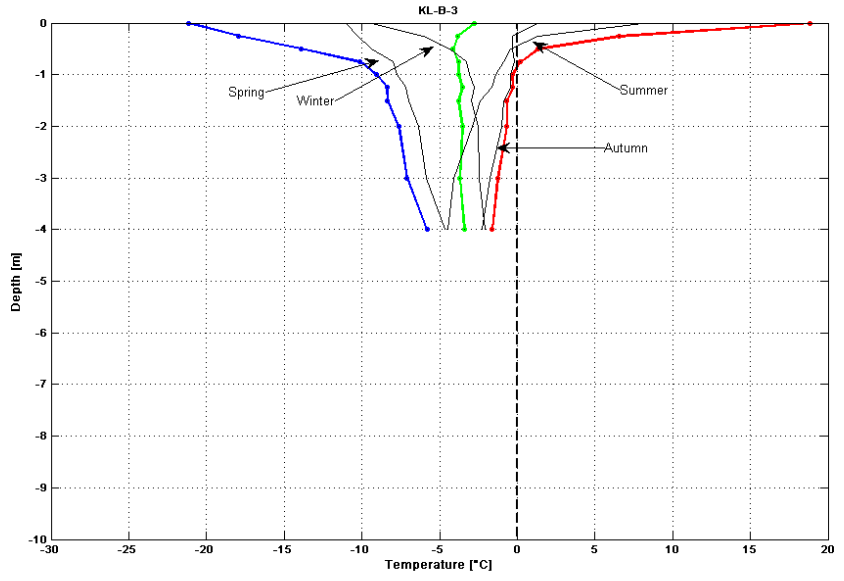

Figure 33 Trumpet curves at the KL-B-3 site.

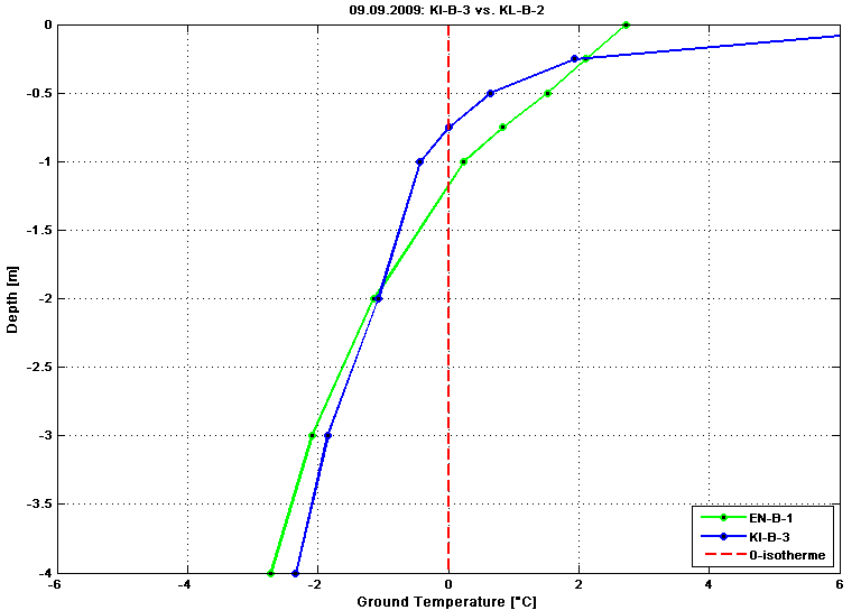

Figure 34 Ground temperatures on the 9th of September 2009 at the two wet locations: KL-B-3 (blue) and EN-B-1 (green).

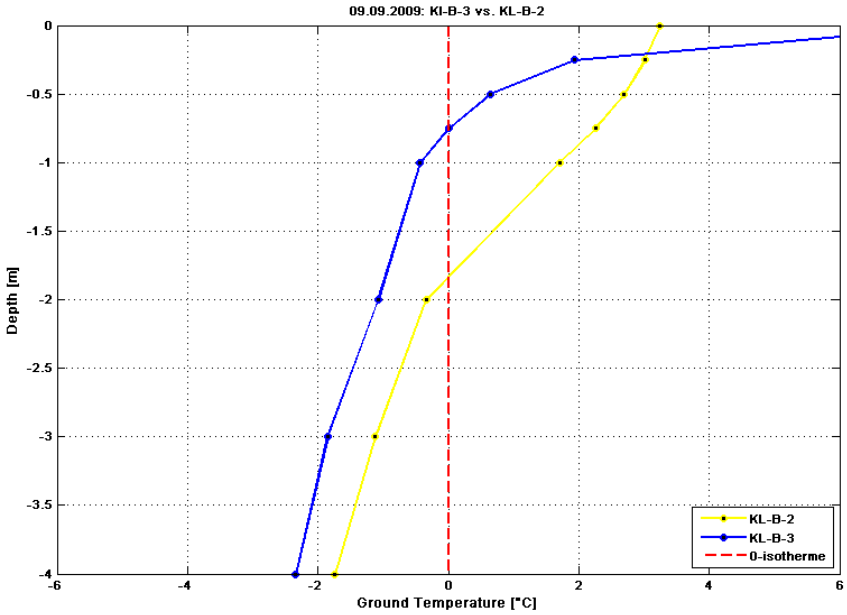

Figure 35 Ground temperatures on the 9th of September 2009 at the two continental locations: KL-B-3 (blue) and KL-B-2 (yellow).